Design of a Sample Acquisition System for the Mars Exobiological Penetrator

May 4, 1988

Submitted to :

Byron L. Swenson
Chief Investigator, Advanced Projects Studies Office, NASA Ames California

Ron Thomson
University of Wisconsin-Madison

Owen Gwynne
Teaching Assistant, University of Wisconsin-Madison

MARS PENETRATOR
DESIGN TEAM 87-88
University of Wisconsin-Madison

MARS PENETRATOR
DESIGN TEAM 87-88
University of Wisconsin-Madison

c/o Ron Thomson
Engineering Mechanics Dept.
College of Engineering
University of Wisconsin - Madison
Madison WI, 53706

May 4, 1988

Byron L. Swenson
NASA Ames Research Center
Moffett Field, California 94035

Dear Mr. Swenson:

Enclosed is our final design. The ideas presented in our December proposal have been refined and improved. We have eliminated much of the excess weight due to gear systems and motors while simplifying the overall operation. Except for two electronic timing devices, the entire system is mechanical in nature. One note of importance, the overall height of the redesign has increased to 6.5 cm and the shell inside diameter is at 10.5 cm, as opposed to the initial estimate of 5.0 cm and 10 cm respectively.

The project appears to be ready for prototyping. Although tests were run to approximate core-grinding, it will be important to run tests using the actual setup. As far as the manufacturing of the prototype here at the University, we would not be able to make the bit or, probably, the gearbox. These would have to be custom built. Unfortunately, due to departmental budgeting beyond our control, it appears as though we will only have about $1800 to assemble the materials. We have not actually looked into costs so this may still be feasible. If all goes well, things might start sometime this summer.

Thanks for the opportunity to work on this project, we enjoyed working with you. Please keep in touch with us on any future developments.

Sincerely,

Mars Penetrator Design Team

Design of a Sample Acquisition System for the Mars Exobiological Penetrator

ABSTRACT

The Mars Exobiological Penetrator will be imbedded into several locations on the Martian surface. It contains various scientific instruments, such as an Alpha-Particle Instrument (API), Differential Scanning Calorimeter (DSC), Evolved Gas Analyzer (EGA) and accelerometers. A sample is required for analysis in the API and DSC. To avoid impact contaminated material, this sample must be taken from soil greater than 2 cm away from the penetrator shell. This study examines the design of a dedicated sampling system including deployment, suspension, fore/after body coupling, sample gathering and placement. To prevent subsurface material from entering the penetrator sampling compartment during impact, a plug is placed in the exit hole of the wall. A U-lever device is used to hold this plug in the penetrator wall. The U-lever rotates upon initial motion of the core-grinder mechanism (CGM), releasing the plug. Research points to a combination of coring and grinding as a plausible solution to the problem of dry drilling. The CGM, driven by two compressed springs, will be deployed along a tracking system. A slowly varying load, ie. springs, is favored over a fixed displacement motion because of its adaptability to different material hardness. However, to accommodate sampling in a low density soil, two dash pots set a maximum transverse velocity. In addition, minimal power use is achieved by unidirectional motion of the CGM. The sample will be transported to the scientific instruments by means of a sample placement tray that is driven by a compressed spring to avoid unnecessary power usage. This paper also explores possible modifications for size, weight, and time as well as possible future studies.

Prepared by:

M. Chun
C. Eble
T. Kilinski
M. Kuehner
M. Wallat
A. Zerfas

MARS PENETRATOR
DESIGN TEAM 87-88
University of Wisconsin-Madison

Table of Contents

Table of Illustrations

Appendix

EXECUTIVE SUMMARY

Penetrators are proposed for subsurface exploration of Mars. Deployed from orbit, they free fall, impact and come to rest one to four meters below the surface.

An integral portion of the Mars Penetrator is the two dedicated sampling devices which gather subsurface material for exobiological analysis. This is accomplished by a series of events, beginning upon impact. First, the communication/power pack, located in the tail section, separates from the forebody and remains on the surface. After the forward section comes to rest, a spring driven core grinder begins its advance toward the penetrator shell. This causes a protective plug to be removed, allowing the sampling system to begin gathering material. After a predetermined distance, the desired sample will have traversed through the bit, and be located in the sample tray. At this time, the tray, following a guide, moves the sample up to a scientific instrument for analysis. A trap door then drops the specimen down a chute for testing in another instrument.

PENETRATOR HISTORY

Penetrators are dart-like objects released from an orbiting vehicle, implanting themselves in the object under study. They are descendants of the Sandia Terradynamic probes that were successfully used for Earth geological surveys. Because of their low cost and high quality data capacity, penetrators have been used by the military for many years. This makes them ideal for planetary missions.

A preliminary design of a penetrator was developed by NASA for the study of a comet nucleus. Their objectives were to implant the penetrator into a comet's center and to :
- determine major elements.
- determine strength and density properties of the outer one meter of the nucleus.
- determine thermal properties.
- use information to increase understanding of the origin, evolution and current state of comets

Another preliminary design has been proposed by NASA for a Mars Penetrator system for subsurface exobiological exploration. Their goal is to set up a global network of seismic, meteorological, geochemical and biochemical observation stations. This penetrator will impact and the afterbody will disconnect and remain on the surface while the forebody continues deeper into the subsurface. An umbilical will connect the two sections. A sampling system in the forebody will obtain Martian soil for experimentation by the penetrator's scientific payload. The afterbody periodically transmits data to an orbiting spacecraft.
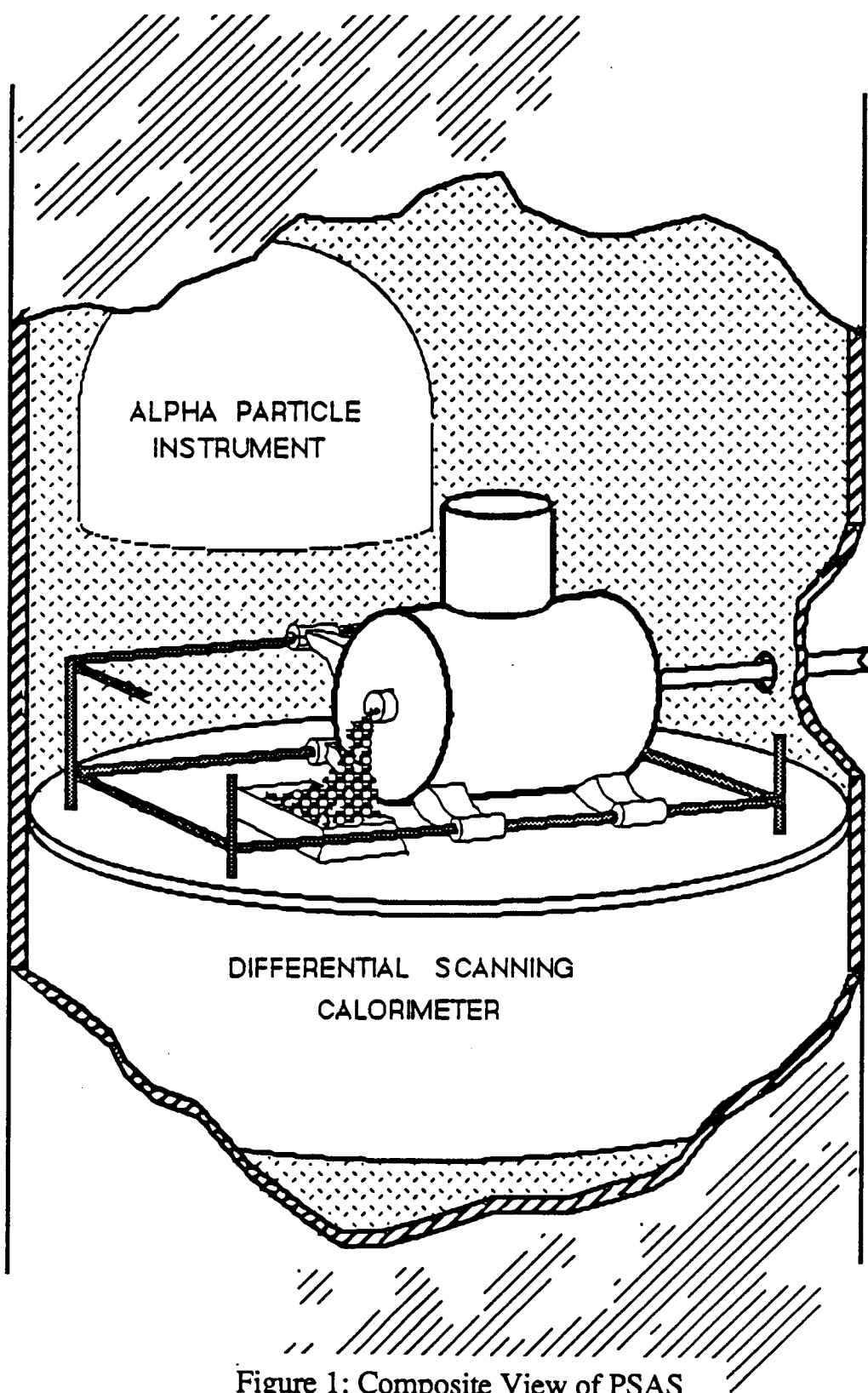
Figure 1: Composite View of PSAS

Driving Springs (Compressed)

Gearbox

Sample Tray Guides

Exit Plug

U-Lever

Driving Springs (Extended)

U-Lever

Protective Impact Mounting
Platform

Bit extended into soil
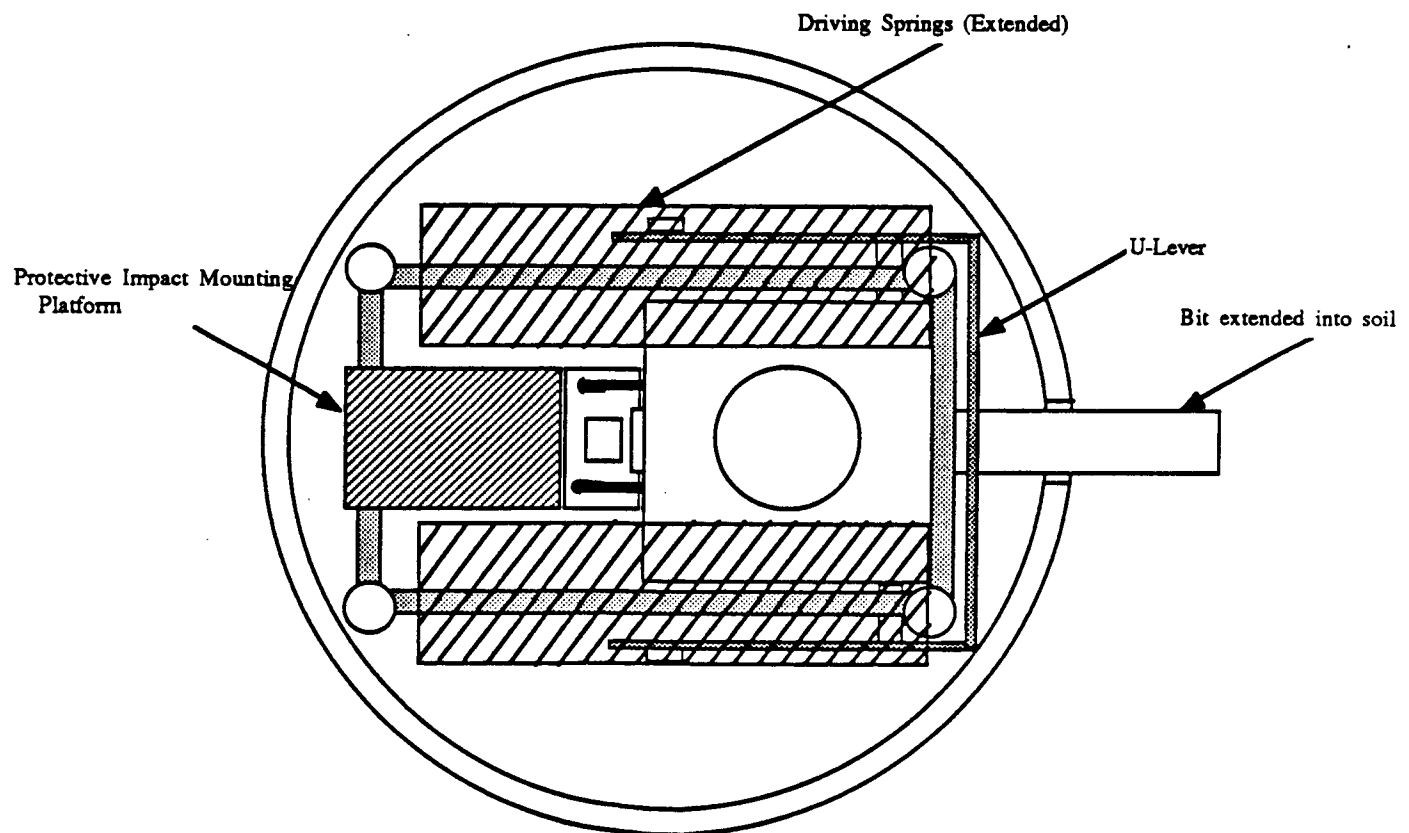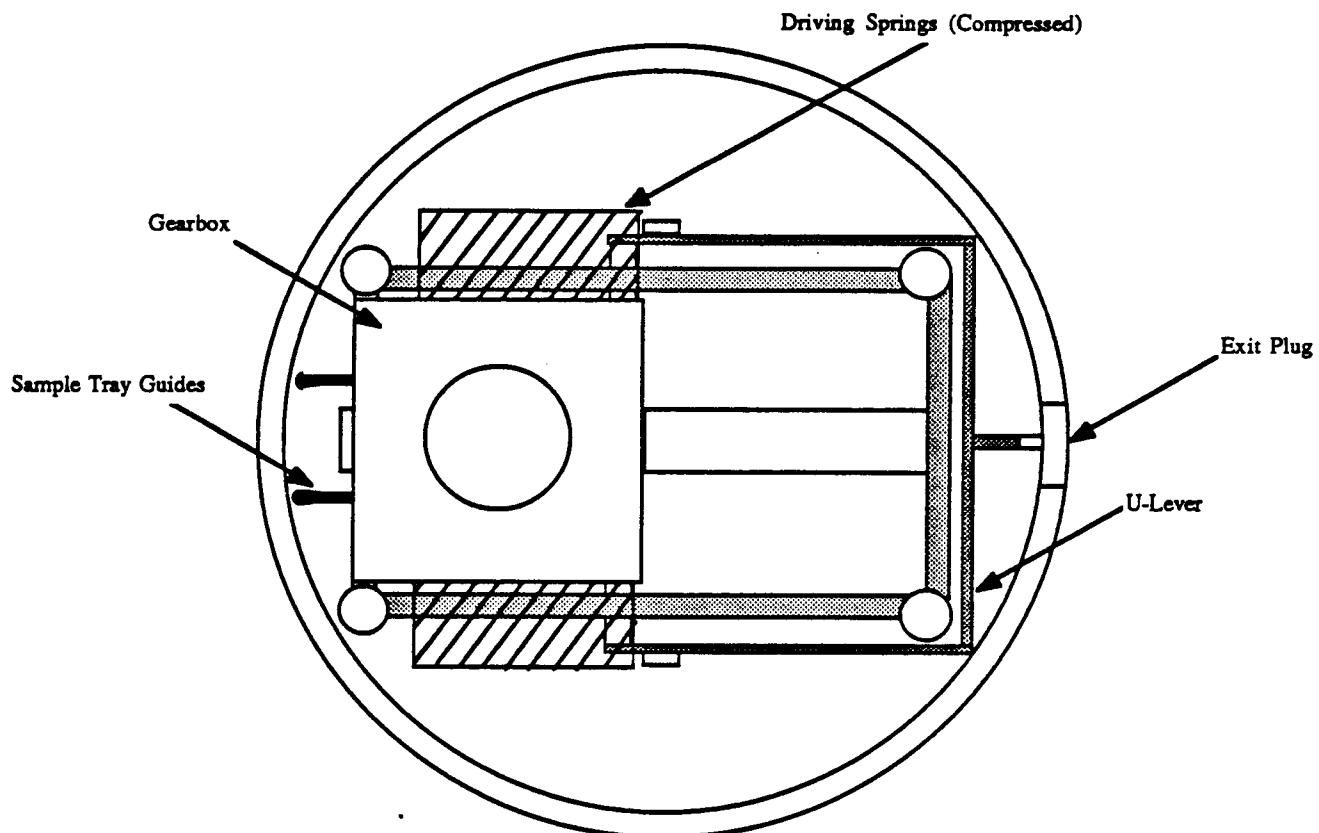
Figure 2: Deployment (top view - initial/final)
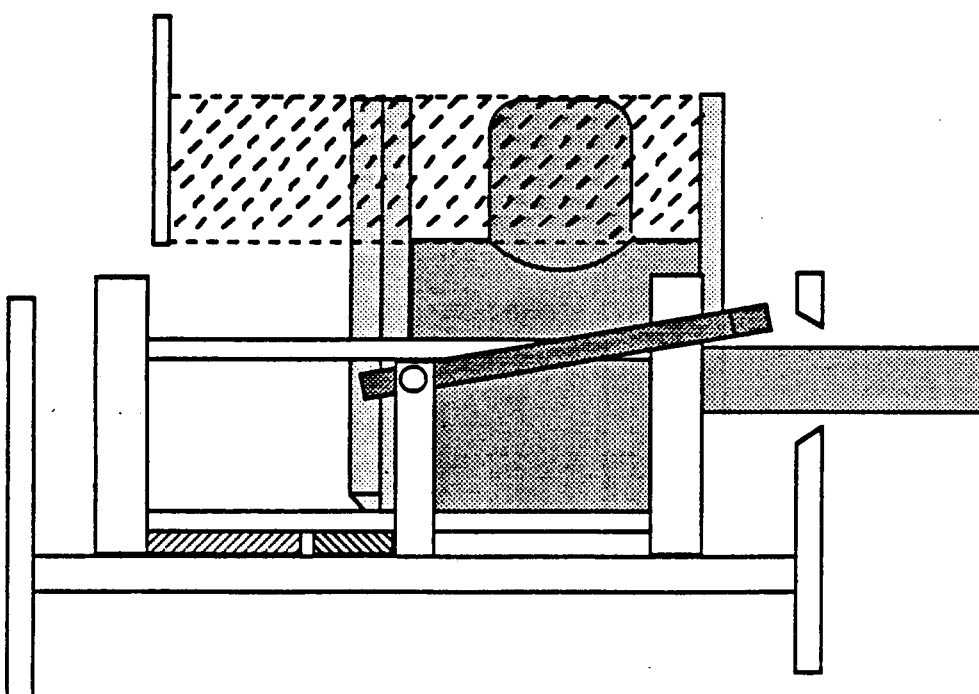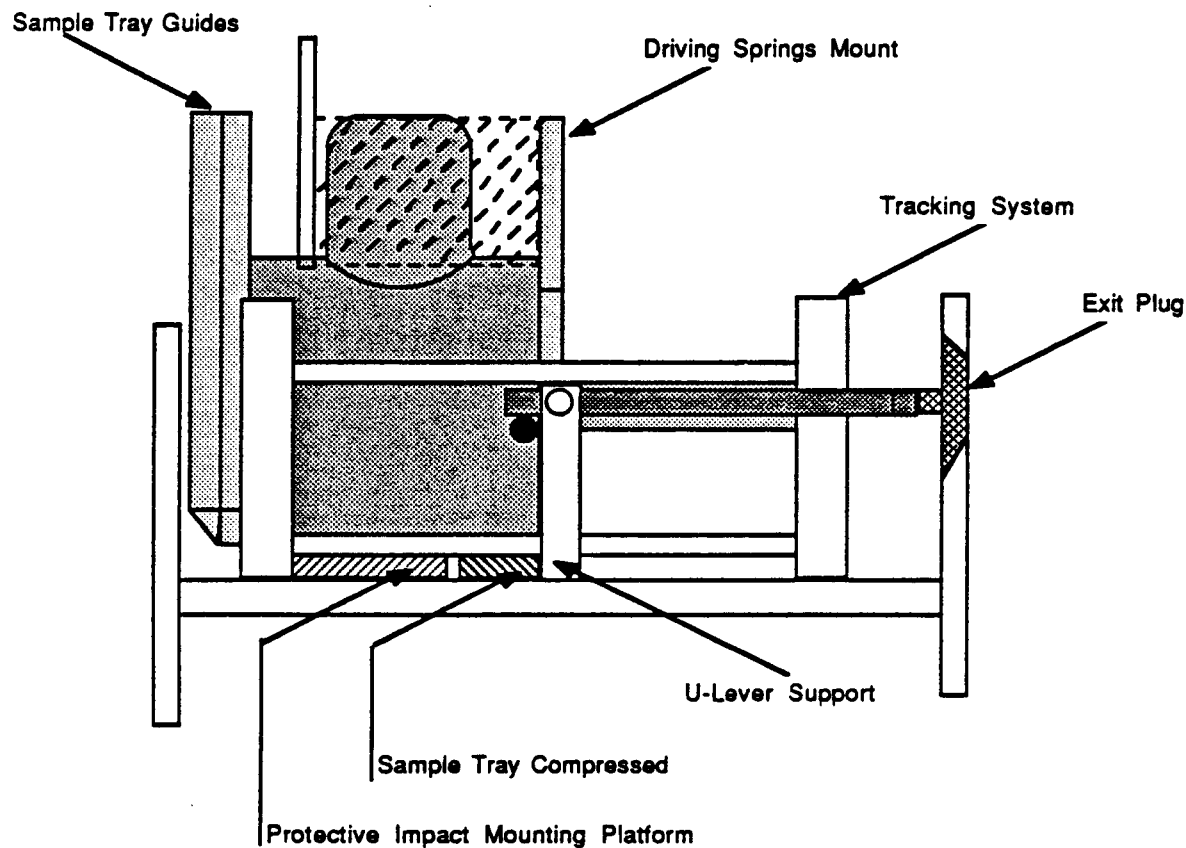
**Figure 3: Deployment (side view - initial/final)**
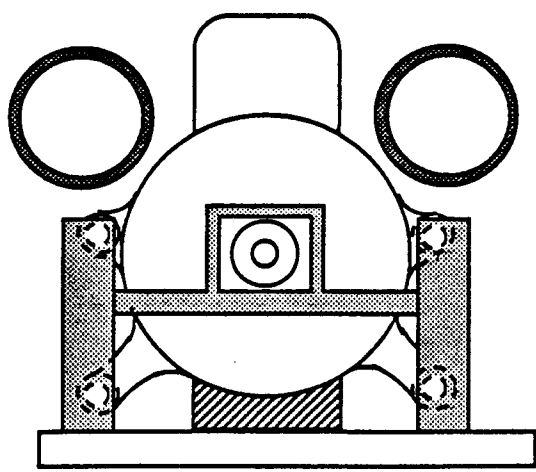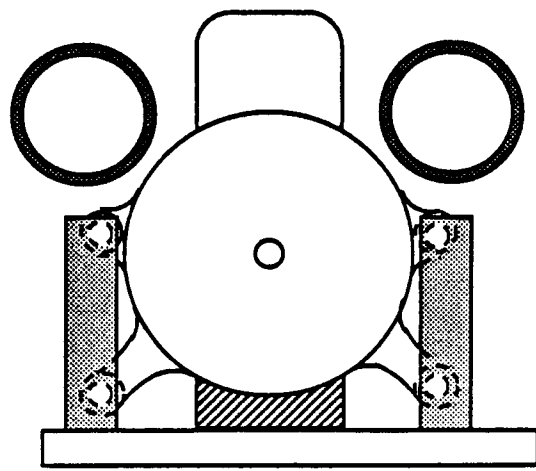
Figure 4: Deployment (rear view and front view)

5

TECHNICAL DESCRIPTION

TECHNICAL PROBLEM STATEMENT

The scientific community is looking at penetrators as an inexpensive but reliable means of subsurface exploration of Mars. The Mars penetrator will be imbedded into various locations on the Martian surface. It contains several scientific packages such as Alpha Particle Instruments, Differential Scanning Calorimeters, and Evolved Gas Analyzers intended for analysis of exobiological data. The experiments require undisturbed samples of the Martian crust; therefore, a method of acquiring these samples has been designed. This report presents a design of a Sample Acquisition Device (SAD) and a fore/after-body coupling for the Mars penetrator.

TECHNICAL MISSION PURPOSE

The purpose of the Mars Penetrator mission is to :
- search for biogenic organic material.
- determine thermal characteristics of Martian subsurface material.
- determine the specific mineral and chemical composition of Martian subsurface.
- use new information to increase understanding of Mars and Earth.

There is evidence that primordial Mars and Earth may have been very similar. An atmosphere of carbon dioxide and nitrogen, moderate surface temperatures, and high geothermal heat flow suggest a primordial Martian biosphere like that developing on Earth. These similarities in addition to an absence of tectonic activity on Mars, seemingly low erosion rates, and low temperatures lead some scientists to believe that Mars may contain the best preserved record of early events on terrestrial planets.

To obtain the above information, the penetrator will carry an Alpha Particle Instrument(API), a Differential Scanning Calorimeter(DSC), and an Evolved Gas Analyzer(EGA). (See Appendix B for further information on the scientific package.)

If the penetrator could be guided to regions where water may have flowed billions of years ago, it could be assigned to detect :
- organic material.
- carbonate and other sedimentary deposits.
- clays/weathered minerals.

A network of penetrators would also allow scientists to determine where future missions, such as the unmanned Mars Rover or a more extensive array of penetrators, should be targeted.

TECHNICAL PROJECT PURPOSE

Our design goal is focused on solving two major problems:

- Maintain rigid coupling between penetrator sections until impact. The afterbody is left at the surface to maintain a communications link to the orbiter, while the forebody continues below the surface to conduct experiments.

- Acquire a pristine sample of the Martian subsurface soil for analysis. The soil within 1-2 cm of the penetrator shell is altered by impact energy in the form of heat and shock waves. Therefore, we must design a system to bypass the contaminated region and return a 10 mg sample of undisturbed soil to the penetrator for analysis.

DESIGN PROBLEMS

A complete design of a Penetrator Sample Acquisition System (PSAS) must address the following problems:

1. General Requirements
   - The size and mass of the system must be designed within the capacity of the penetrator.
   - A suspension system must be designed for PSAS to protect it from impact while offering rigidity during deployment and sampling.

2. Deployment
   Deployment of a Sample Acquisition Device requires an opening of the penetrator exterior shell after impact. In the past, complications have arisen from impact effects. In particular, contamination and blockage of the opening have occurred from smearing of the exterior coating. Also the hole must not jeopardize the integrity of the shell, while still provide clearance for the Core Grinder Mechanism (CGM) bit to exit the shell.

3. Sample Acquisition Device (SAD)
   The main objective of SAD is to extend into the surroundings and gather a sample that is unaffected by impact and also unaltered by the sampling technique. This must be done for materials ranging in density from fine regolith to volcanic rock. Since the material in the immediate vicinity of the penetrator is contaminated by the impact, SAD must clear a path past this layer to an unaffected sample. Also of concern is the effect of heat on the composition of the sampled material.

7

4. Sample Placement

Once the sample is inside the penetrator it must be introduced to two separate scientific packages, the API and the DSC.

5. Fore/Afterbody Coupling

There must be a rigid coupling between the fore and after sections of the penetrator during its transportation to Mars and its free fall from orbit. This connection must allow for a controlled decoupling upon surface impact.

PROJECT GOALS

This design focuses its attention on solving one major problem; obtaining a sample for experimentation. The intention of this study is to obtain solutions to the following design problems:

1. Fore/Afterbody Coupling (FAC)

FAC will keep the nose and tail sections of the MEP rigidly connected throughout the mission until impact. Upon impact it will allow the two sections to separate.

2. Sample Acquisition Device (SAD)

SAD must be designed to operate within the design specifications for sampling, collecting, and returning a specimen.(see Appendix A)

3. Sampling System Suspension (SSS)

The purpose of the suspension plate is to insure that SAS survives the impact and remains aligned within the penetrator shell.

4. Deployment of SAD

This involves determining a method of getting SAD from the inside to the outside of the penetrator shell.

5. Sample Placement

The sample must be deposited into the testing equipment for analysis.

COMPONENT DESCRIPTIONS

A. FOREBODY/AFTERBODY COUPLING

The MEP is composed of two sections which separate at impact. The forebody/afterbody coupling keeps the two sections rigidly connected throughout the space flight and descent through the Martian atmosphere. It then allows for controlled separation upon impact so that the nose section may continue below the surface, leaving the afterbody above.

The forebody is a cylindrical shell of inside radius 5.25 cm. It fits over a cylindrical shell of outside radius 5.25 cm which extends 5 cm from the tail section. Three shear pins, 3 mm square in cross section, are used to couple the two sections. The pins extend from the outer shell through grooves in the inner shell. A lock prevents rotation of the shells relative to each other. As the wider tail section impacts, an acceleration increasing to more than 1500 g's will be imparted to the tail section. When the acceleration reaches 400 g's, the pins will shear off, allowing separation.

The locking mechanism consists of a cantilever beam welded to the interior of the inner shell. The free end of the beam extends into the horizontal slot that the pin slides through during assembly. As the pin slides through the slot, it contacts the beam. The beam is elastically deflected when the pin is forced past and snaps back to its original position behind the pin, thereby locking the pin in place. A second lock is included as a backup. No allowance for unlocking the pins has been made because the need is not foreseen and it would add unnecessary complexity to the design. A titanium alloy is the material of choice for the shear pins because it retains its ductility at the low temperatures to be encountered. A ductile material will give a clean shear failure at a predictable load.


Figure 5: Shear Pin

9
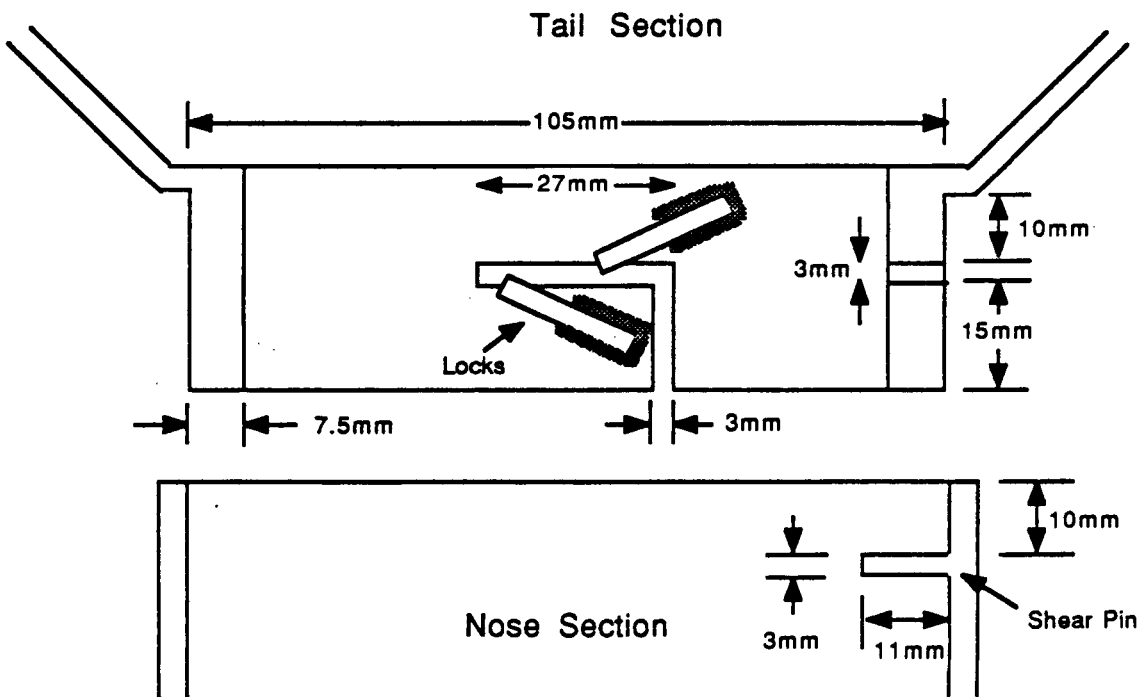
B. SUSPENSION SYSTEM

The main purpose of SSS is to support the PSAS and testing equipment within the penetrator shell. It must withstand a 400 g impact force and keep the PSAS in proper alignment after impact.

The suspension system consists of two flat circular plates. These plates are spaced 6.5 cm apart vertically with a thickness of 0.5 cm and a diameter of 10.5 cm. There is also a hole centered 4.4 cm from the inner wall of the shell in each plate. The hole in the upper plate allows the sample to be scanned by the API, while the hole in the lower plate allows the sample to be transferred to the DSC. The plates will be circumferentially welded to the shell along a top or bottom edge. All welds use a gas tungsten-arc welding process.

The main concern of this project was the strength and stability of the plates and the strength of the welds at a 400 g impact. No information could be found on the weld strength of Ti-5Al-2.5Sn, which is proposed for the penetrator shell, however, tests have been performed on the weldability of Ti-7Al-2Cb-1Ta. For this reason Ti-7Al-2Cb-1Ta data was used to model the material used in the plates, assuming that the difference between the alloys is negligible. The flat plate theory was used to predict the deflection of the plate. The deflections turn out to be negligible (see calculation). To find the strength of the material and the welds, the shear was calculated along the circumference. The maximum calculated shear at impact is 357 MPa. The shear yield strength of Ti-5Al-2.5Sn alloy is 517 MPa (510 MPa in a weld).
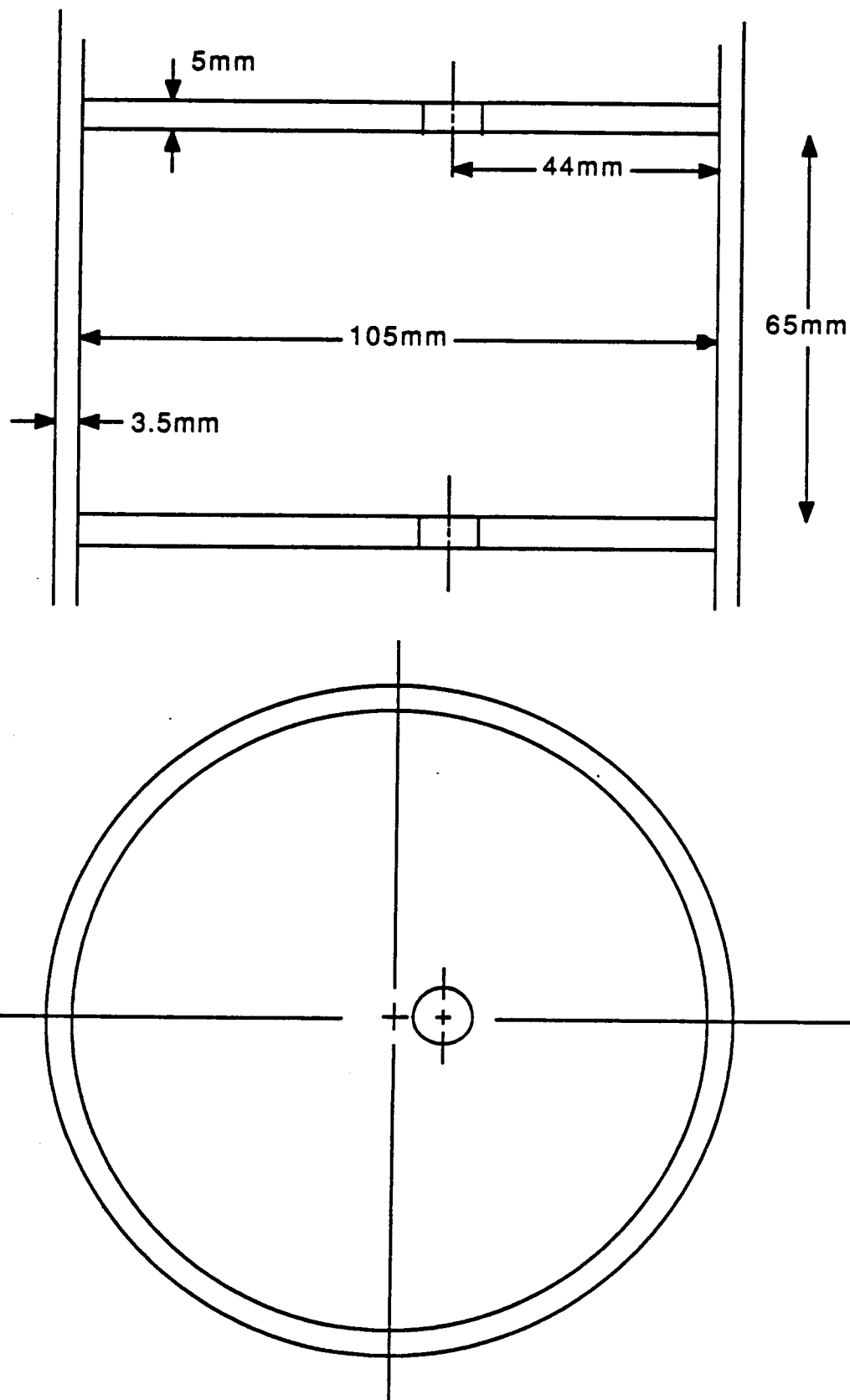
Figure 6: Suspension Plates

11

C. PLUG

To avoid contaminated material from entering the penetrator, a titanium plug occupies a hole in the penetrator wall. A diameter of 1 centimeter is chosen to retain a reasonable dynamical stress concentration while allowing for proper clearance of the 9 millimeter diameter bit (see Pao). To insure plug removal, the following features have been incorporated into the design:
- The plug is coated with a friction reducing surface.
- A unique cross-section facilitates removal.
- A spring (see Appendix D-3) attached to the back of the plug provides an additional force for removal.
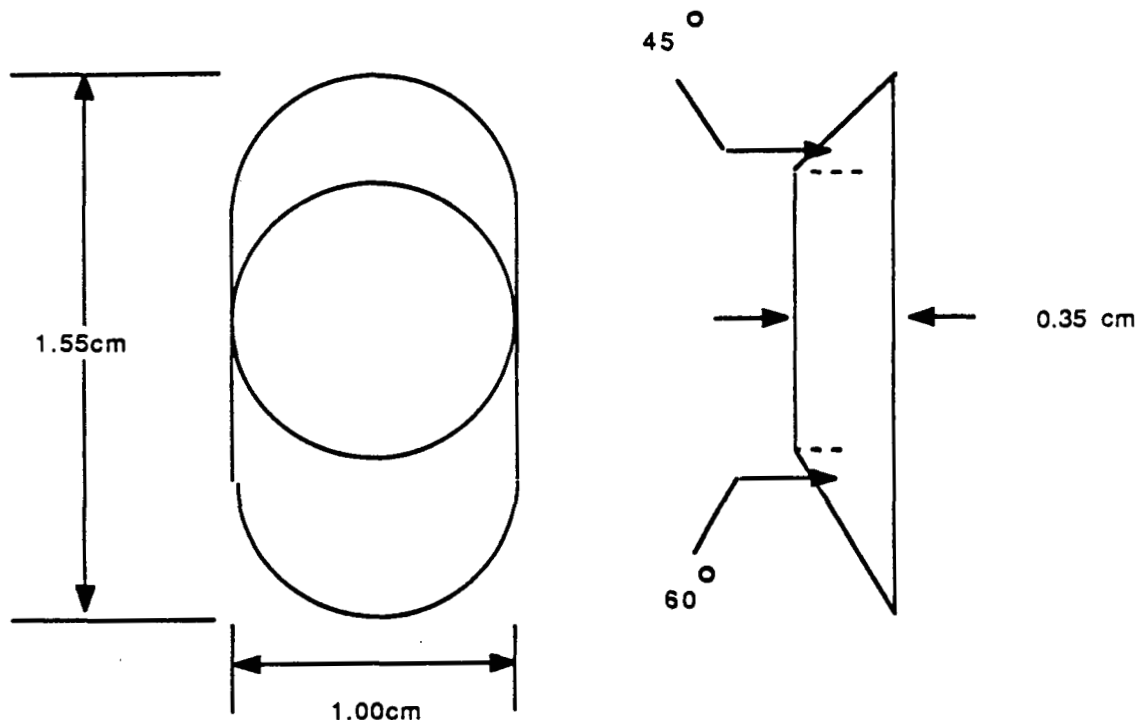

Figure 7: Portal Plug

D. U-LEVER

To initiate plug removal, a lever attached to the tracking system, initially holding the plug in the wall, pivots away from the plug. This allows the plug spring to remove the plug. This U-Lever is designed to support its own weight during impact as well as resist buckling from the plug spring force.

During impact, the U-Lever is supported by a brace on the tracking system as well as two pegs on the sides of the gearbox. The motion of the gearbox initiates the movement of the U-Lever. This occurs when the two pegs on the gearbox move past the lever's pivot point located on two separate supports. At that point, the pegs will no longer constrain the lever against rotation. A spring at the plug opening end will then pull the U-Lever vertically away from the plug.
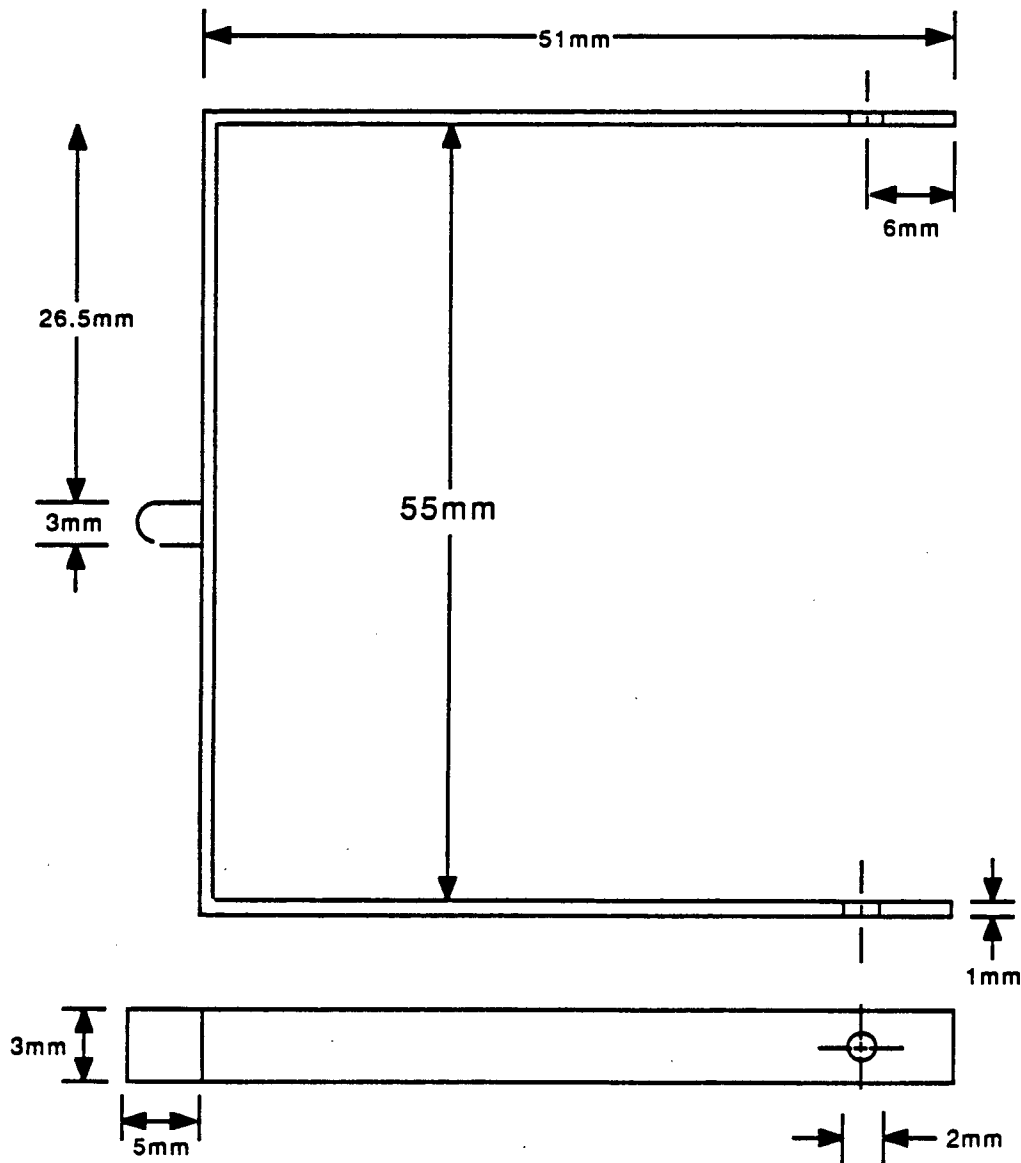
Figure 8: U-Lever

E. TRACKING SYSTEM

The tracking system is a long rectangular box skeleton (30 mm by 40 mm by 80 mm) with the beam members constructed of a titanium alloy coated with teflon as a friction reducing agent. The tracks provide rigidity and guidance for the core-grinder assembly.

Maintaining the alignment of the CGM is a major concern. Two of the problem areas are impact loads and operational vibrations. The impact loads can be divided into two cases, transverse and longitudinal. Transverse loads are carried by the track's beam members (3.1 mm diameter) (Appendix D-2) while the pure axial forces are transmitted through the Protective Impact Mounting Platform (PIMP). The amplitudes of the operational vibrations due to motor imbalance, are assumed negligible in comparison with the impact loads. Guidance will be accomplished by eight arms and sleeves attached to the core-grinder housing which guide the assembly. The tolerance between the stabilizer sleeves is 0.01 mm insuring that the oscillations due to the CGM operation will not be critical with respect to the deployment hole alignment. The forward motion of the motor/gearbox arrangement will be halted by two stops located on the rails. To allow time for the plug to be fully removed, the spring-dashpot driving mechanism will delay the initial forward motion of the CGM.
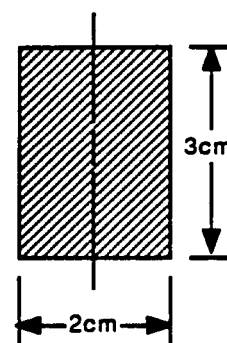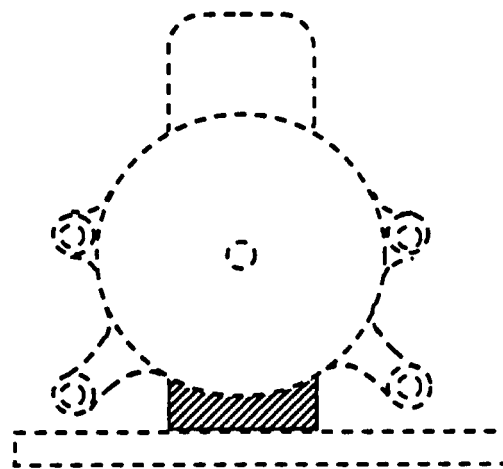
Figure 9: Protective Impact Mounting Platform (PIMP)

1.5 mm

3.3 mm

1.5 mm

4.0 mm

4.0 mm
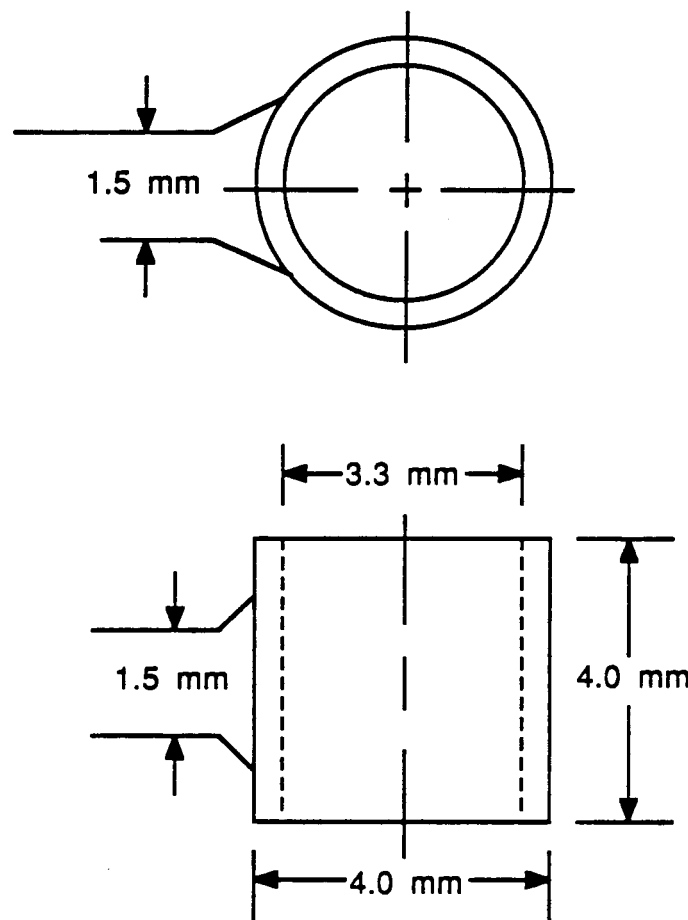
Figure 9a: Stabilizer Arm

F. DRIVING SPRINGS

The core-grinder mechanism is driven forward by springs parallel to the tracking system. These springs remain compressed until deployment of the assembly. Initially they will be held compressed by a solenoid switch and plate. Springs were chosen for their loading characteristics; namely that over the total distance travelled, the change in spring force can be small. Experimental data shows that a back force of about 30 pounds is sufficient for core-grinding for the hardest expected material. Therefore the designed spring forces will vary from 50 to 15 pounds during operation. Under the spring load, the core-grinder will move forward only as fast as it can grind the soil, thus eliminating the worry of bucking or stalling of the bit.

In addition to springs, a dash pot provides a translational speed control on the CGM. This feature delays the bit from hitting the opening before the plug can be removed. Speed control is also important in the case where the surrounding material is very light, in other words, when the soil offers very little resistance to the bit. The damping coefficient for the dash pots was calculated to insure flow rate through the bit for the lightest possible material expected. For this case, we used a density of powered chalk as an absolute lower limit, but realistically, we do not expect to encounter such a light material. Whereas more conventional systems use a fixed-rate, our design combines a quasi fixed load and a limiting translational rate which makes it very adaptable to soil hardness. Thus, our CGM will work just as well in loose sand as in basalt.

G. DRILL BIT

The drill bit used in the CGM is a composed of two hollow bits, one placed inside the other. The outer bit is made of a Titanium alloy, and is fitted with a tapered, diamond impregnated cutting end. The purpose of this bit is to chip at the soil/rock until it is small enough to be passed through the inner bit. The tapered entrance guides the sample to the inside of the bit while providing an excessive volume to minimize material cavities. The outer bit is the load-bearing bit; that is, it is subjected to the bending and twisting forces associated with torsion.

The inner bit is a non-load bearing bit. Its purpose is to move the sample back into the penetrator shell where it can be deposited into a tray for analysis. The inner surface of this bit is fitted with a left-handed helical thread (pitch = 5.500 mm ; thread angle = 45°) (Appendix D-4). The goal of this set-up is to pass the sample through the entire length of the inner bit (8 cm) for a 0.5 cm forward progress of the system.

The sample passed through the bit must be unaltered chemically and physically intact. This poses a problem of contamination by heat generation and by contact with altered material still remaining in the inner bit. The flow contamination problem is solved by effectively passing enough sample through the bit to "clean out" the altered material before passing the sample to be analyzed. The heat generation due to CGM operation is remedied by the gas buffer between the two bits and the thermal conductivity of the titanium alloy. The temperatures in the interior of the inside bit were shown to be very close to that of that of ambient surroundings. (See Appendix G)
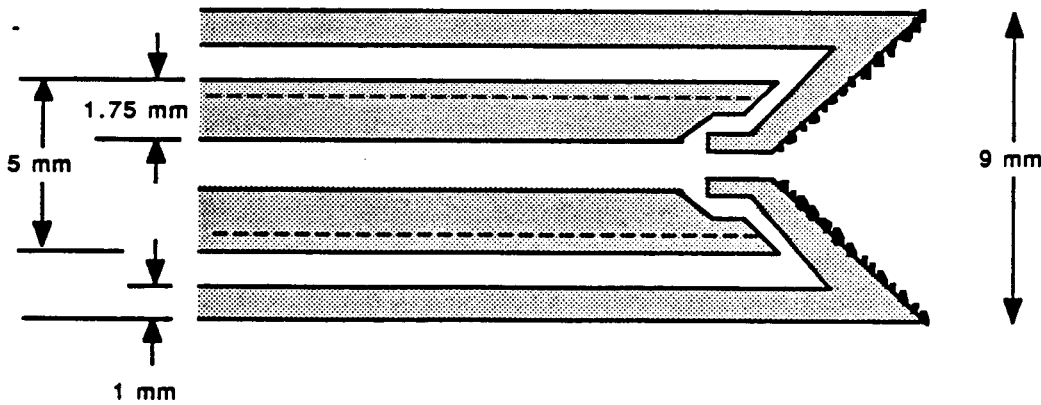

Figure 10: Drill Bit

H. GEARBOX/MOTOR ASSEMBLY

A counter-rotating gearbox is used to provide the necessary speed and rotation directions of the bit assembly. Size and weight limitations restrict the gear box height and length to 4 cm. The motor used to drive the drill bits is positioned directly on top of the gear box. The motor casing is set into the gear box via slotted keyway. The matching surfaces are then welded together to eliminate the possibility of disconnection or slip during use.

Three beveled gears provide the counter-rotation action. The motor is attached directly to the center gear and rotates with an outward moment. An identical gear (ratio 1:1) is meshed with the driven gear and is connected to the outer bit. Thus, the outer bit rotates in the same direction and speed, providing the cutting rotation of 360 rpm (neglecting losses). The inner bit is connected to a smaller gear (ratio 1:4) and meshed to the opposite side of the driven gear. This orientation drives the inner bit at 1440 rpm in the opposite direction (inward moment). Lubrication of the gears is accomplished by the use of a bonded solid film lubricant, eg. Electro-film 77-S. This lubricant is especially useful for hard metals and high loads.
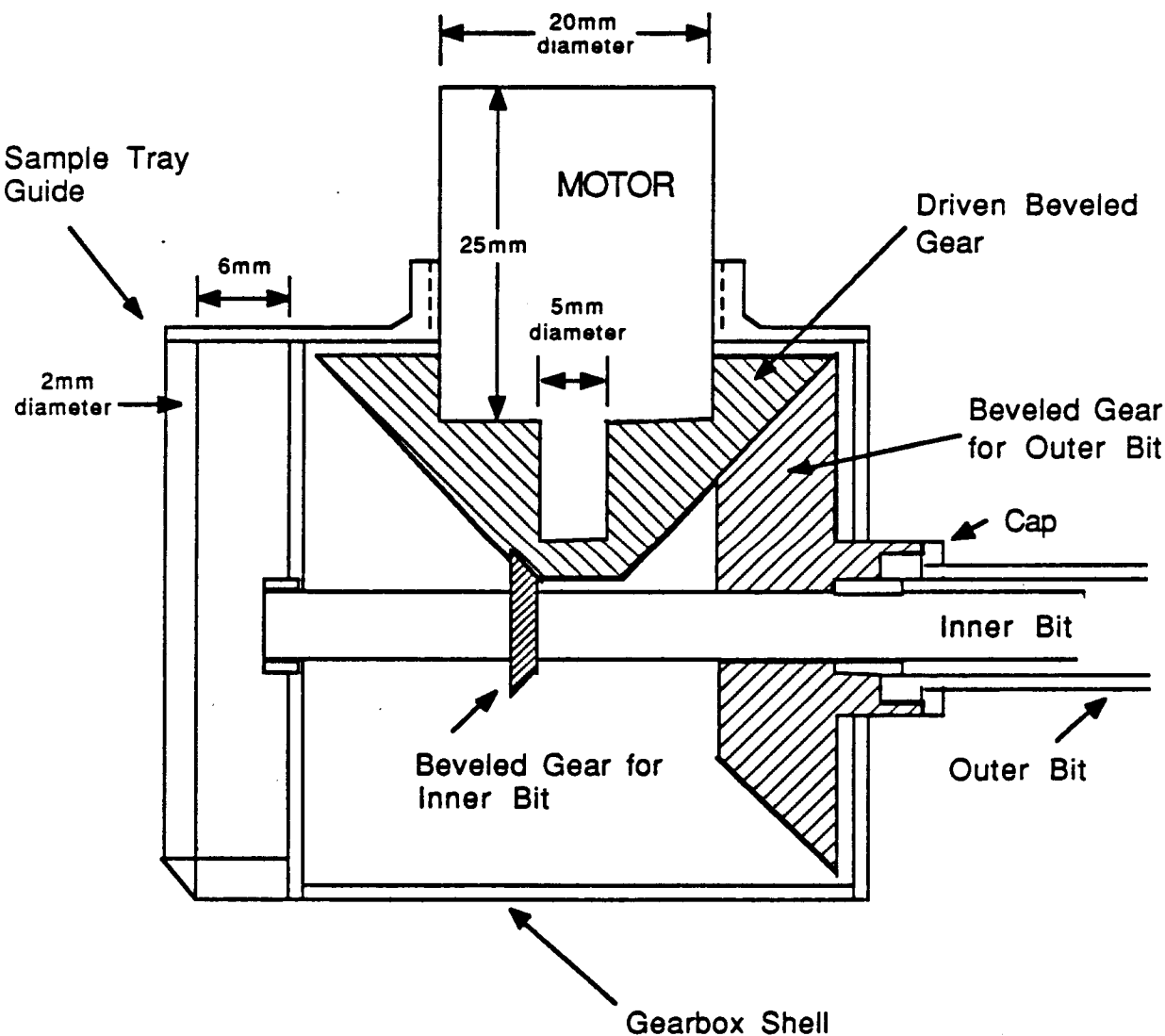
Figure 11: Gear Box Cross-Section
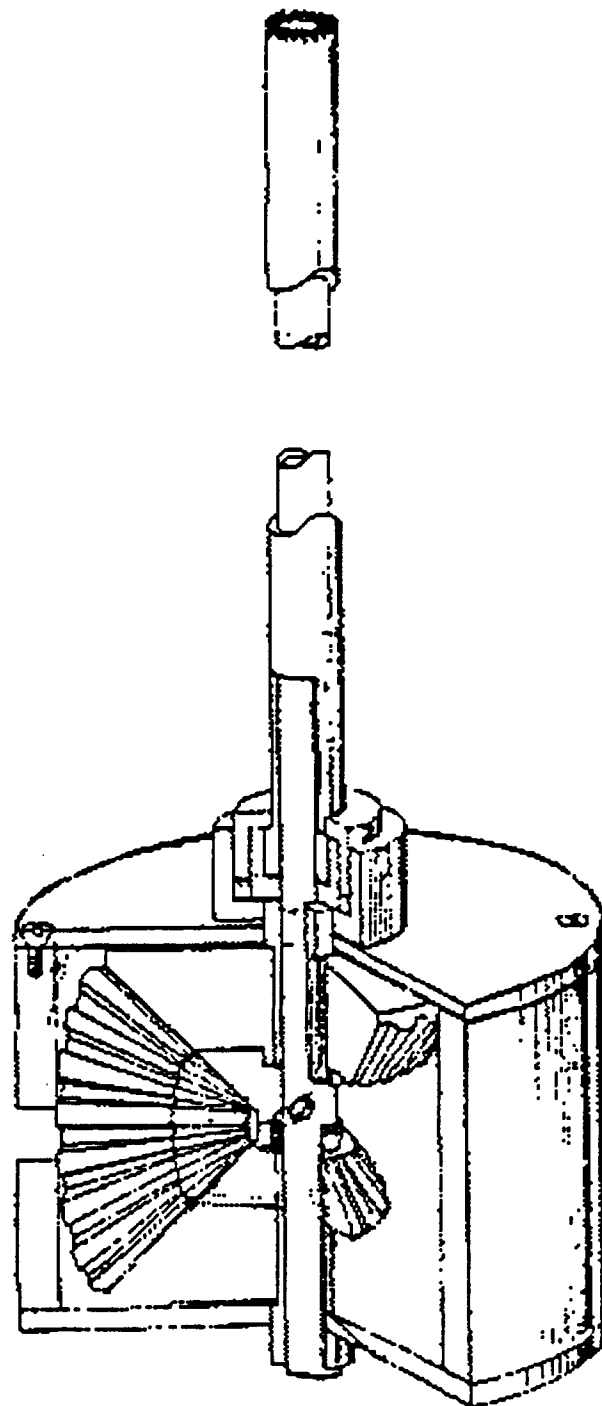
Figure 11a: Gearbox/Bit Assembly

19

I. SAMPLE PLACEMENT

The sample placement device is a tray moved by a spring to the testing equipment. It consumes very little power, only enough for a small timing device. The tray has dimensions of 1 cm deep by 2 cm wide and 1 mm thick with a sunken container (0.5 cm by 0.5 cm) that holds the sample. There are alignment grooves on either side of the sample dish that restrict the tray to vertical movement. These guides extend from, and move with the the back of the gear box.

The tray is driven by a conical, brass alloy spring (ASTM B 134), of rate 0.127 lb/in. The spring has a base diameter of 1.5 cm and a minimum diameter of 0.707 cm with the spring has a full length of 7 cm and a compressed height of .5 cm. The recessed portion of the tray fits inside the top of the spring, while the base of the spring is attached to the base plate of the SAD suspension around the hole, above the DSC. A flexible chute is attached inside the spring coils that will extend 6.5 cm (distance to the API). The recessed base is hinged on one side and secured in place by an electronic lock. Testing the sample requires three movements: (1) through the core-grinder bit and out the back of the gear box into the sample tray, (2) up to the API located above SAD, and (3) down to the DSC located below SAD.

This motion is accomplished with a spring, a timing lock, a hinge, and a cylindrical chute. The spring and guides move the sample up to the API, extending the chute within the spring. The timing mechanism will allow time for analysis, then it will drop out the bottom of the tray. The sample will then fall down the chute due to gravity, to the DSC for analysis. The spring and chute remain extended.
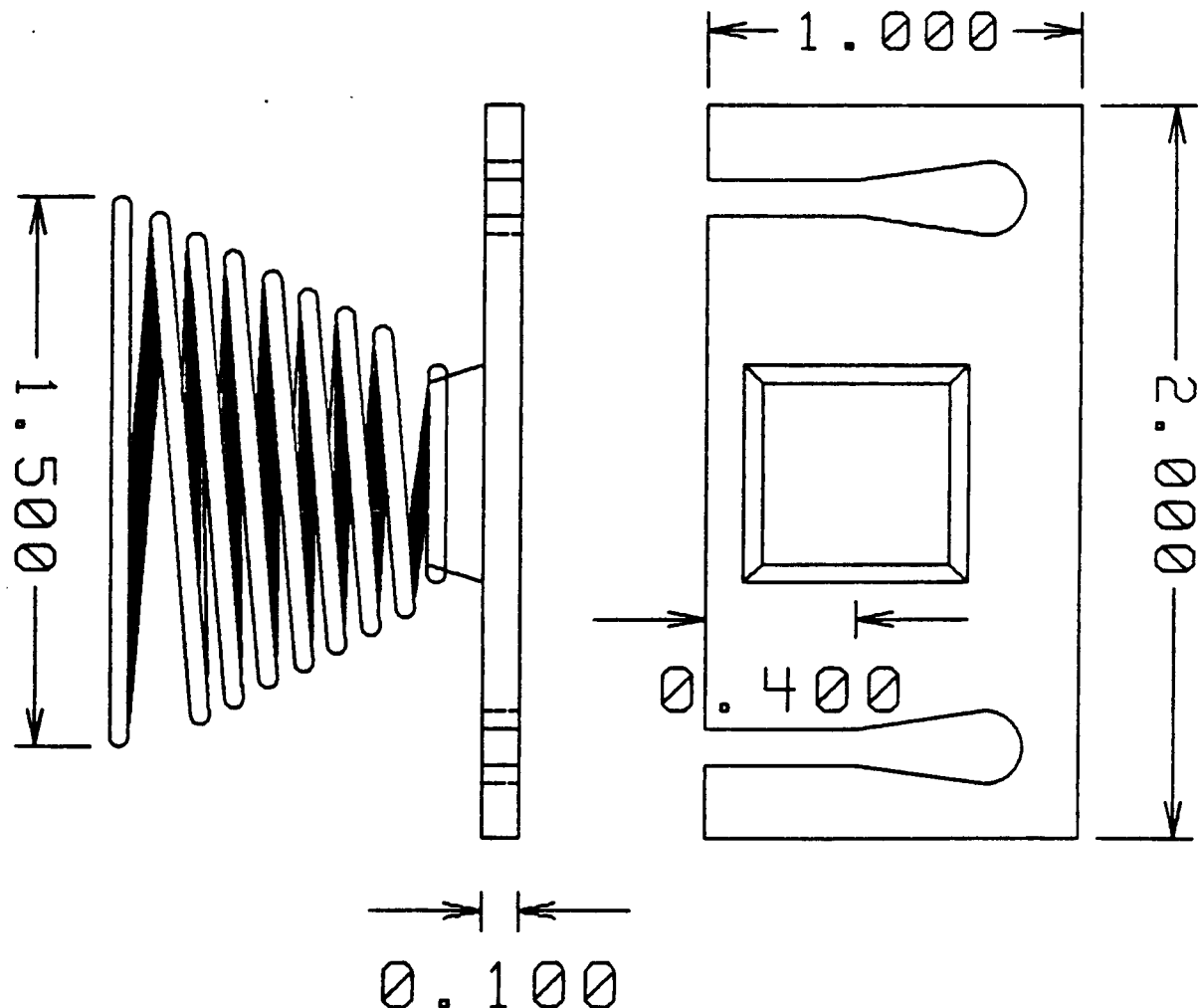

Figure 12: Sample Tray (top view and side view)
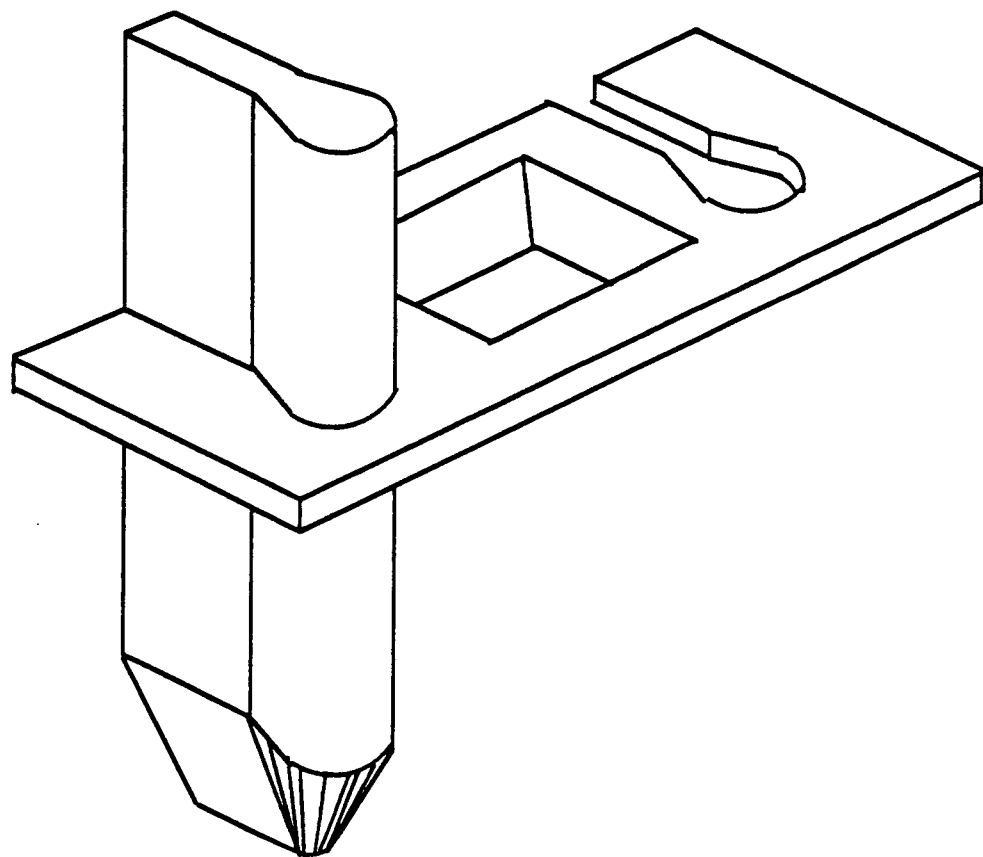
Figure 13: Sample Tray / Guide Post Interface

```
┌─────────────────────────────────┐
│  4-12 Mars Penetrators in an Orbiter Vehicle │
│       are Launched from Earth    │
└─────────────────────────────────┘
                 │
                 ▼
┌─────────────────────────────────┐
│   Orbiter reaches Mars and drops │
│   penetrators at various locations│
│       on the Martian surface      │
└─────────────────────────────────┘
                 │
                 ▼
┌─────────────────────────────────┐
│  Penetrator impacts surface.  Fore and │
│  Afterbody seperate by controlled failure │
│          of shear pins            │
└─────────────────────────────────┘
                 │
                 ▼
┌─────────────────────────────────┐
│   Forebody comes to rest 1-4 meters │
│         beneath the surface       │
└─────────────────────────────────┘
                 │
                 ▼
┌─────────────────────────────────┐
│ Motor is activated and CGM begins its movement │
│      along the track toward the shell │
└─────────────────────────────────┘
                 │
                 ▼
┌─────────────────────────────────┐
│  Motor moves past pivot point of U-lever │
│        and allows U-lever to rotate │
└─────────────────────────────────┘
                 │
                 ▼
┌─────────────────────────────────┐
│     Plug is removed from portal  │
│           by  plug spring         │
└─────────────────────────────────┘
```

Figure 14: PSAS Deployment Flowchart (1 of 2)
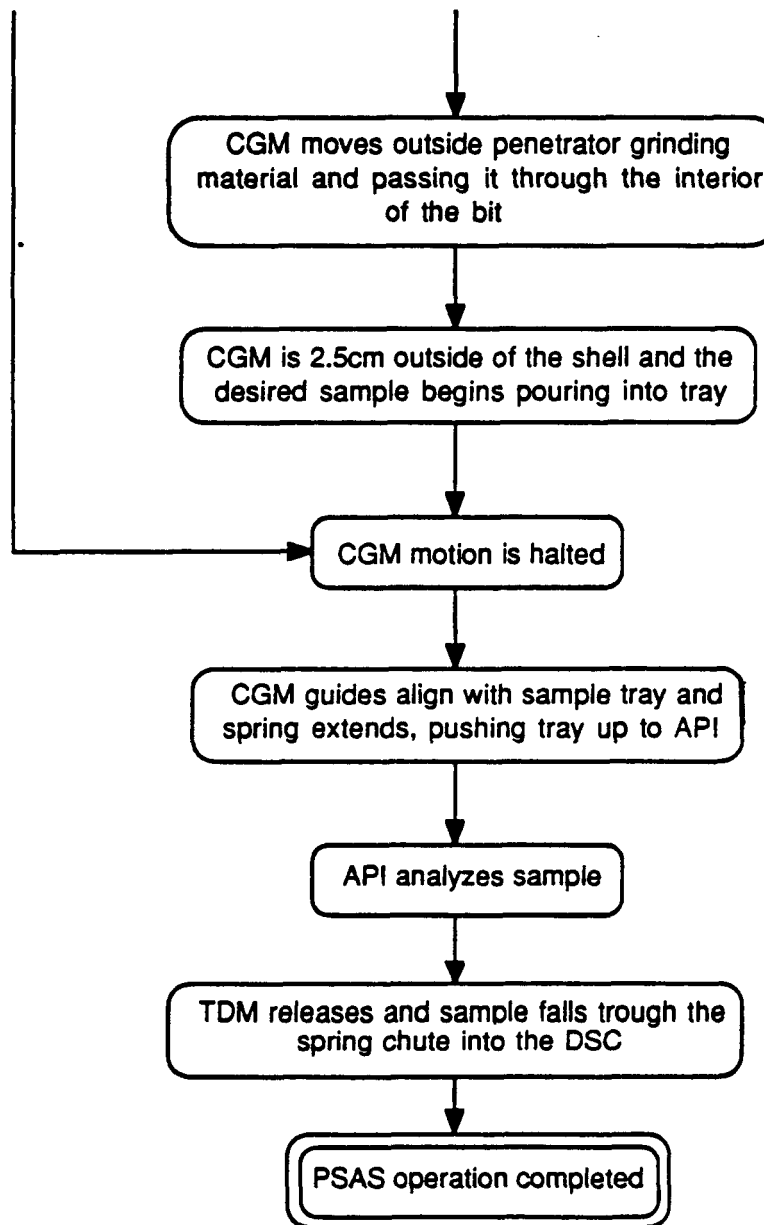
Figure 15: PSAS Deployment Flowchart (2 of 2)
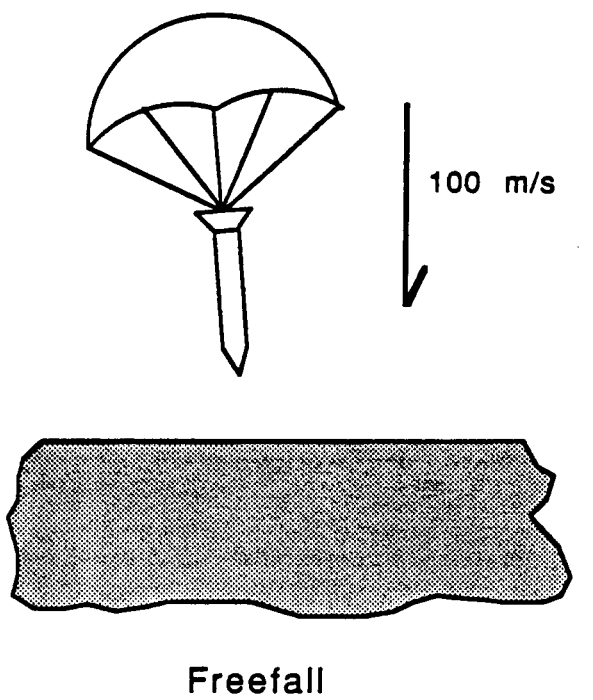
The flowchart contains the following steps:

- CGM moves outside penetrator grinding material and passing it through the interior of the bit
- CGM is 2.5cm outside of the shell and the desired sample begins pouring into tray
- CGM motion is halted
- CGM guides align with sample tray and spring extends, pushing tray up to API
- API analyzes sample
- TDM releases and sample falls trough the spring chute into the DSC
- PSAS operation completed
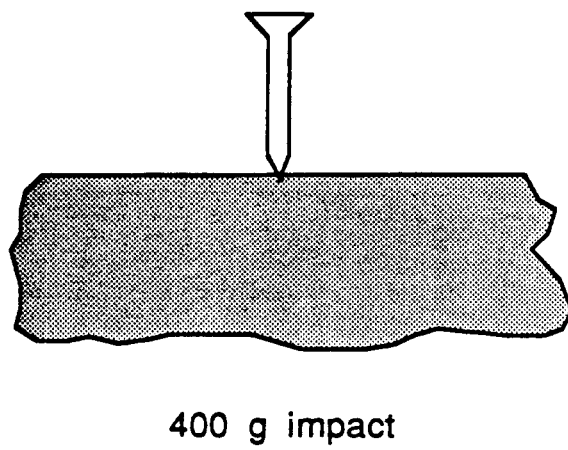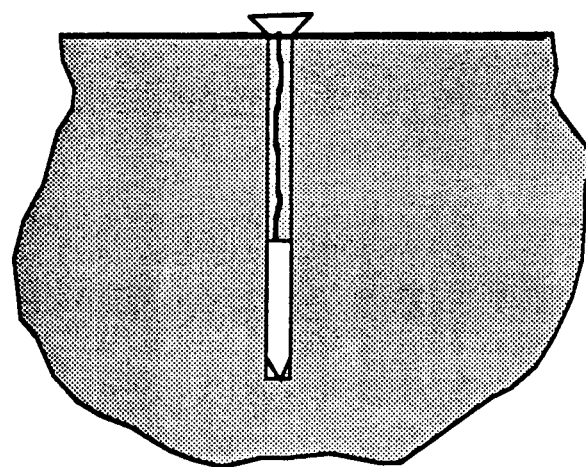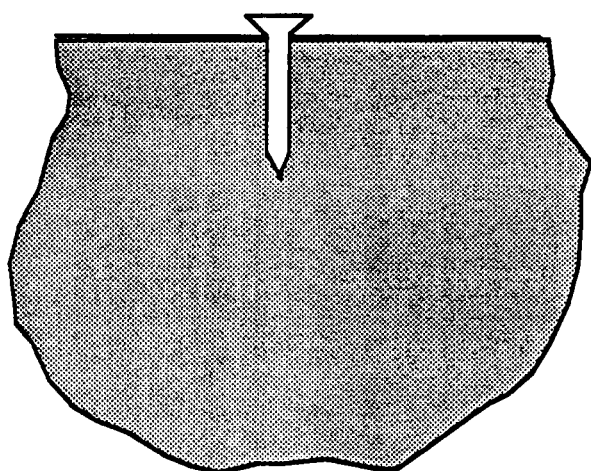
Figure 16: Illustrated Time Sequence (1 of 5)

APT

U-Lever
Pivot Point

DSC
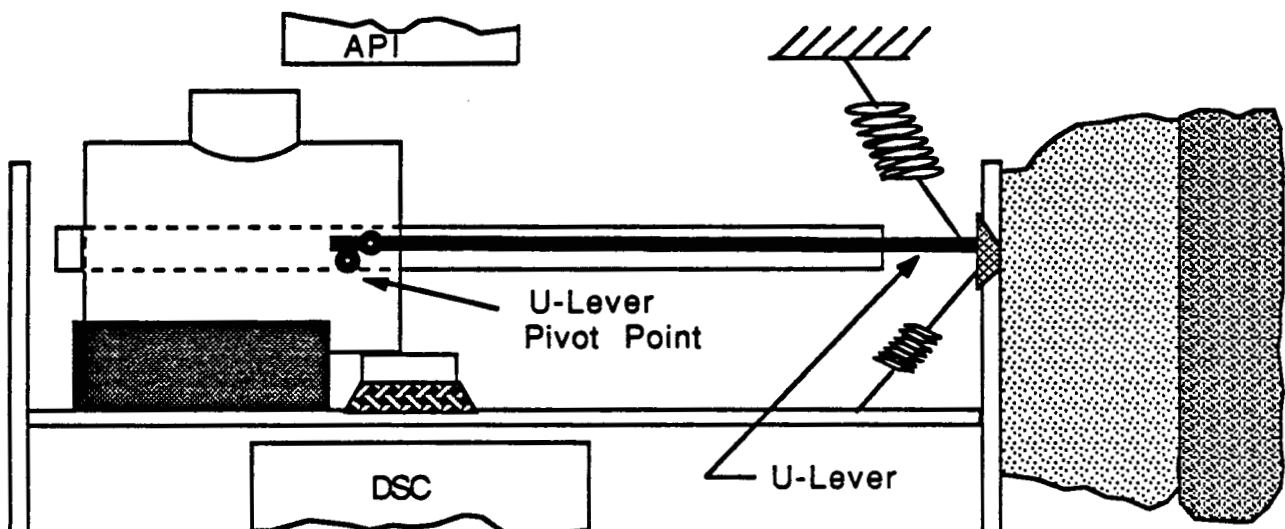
U-Lever

Impact configuration

APT

DSC
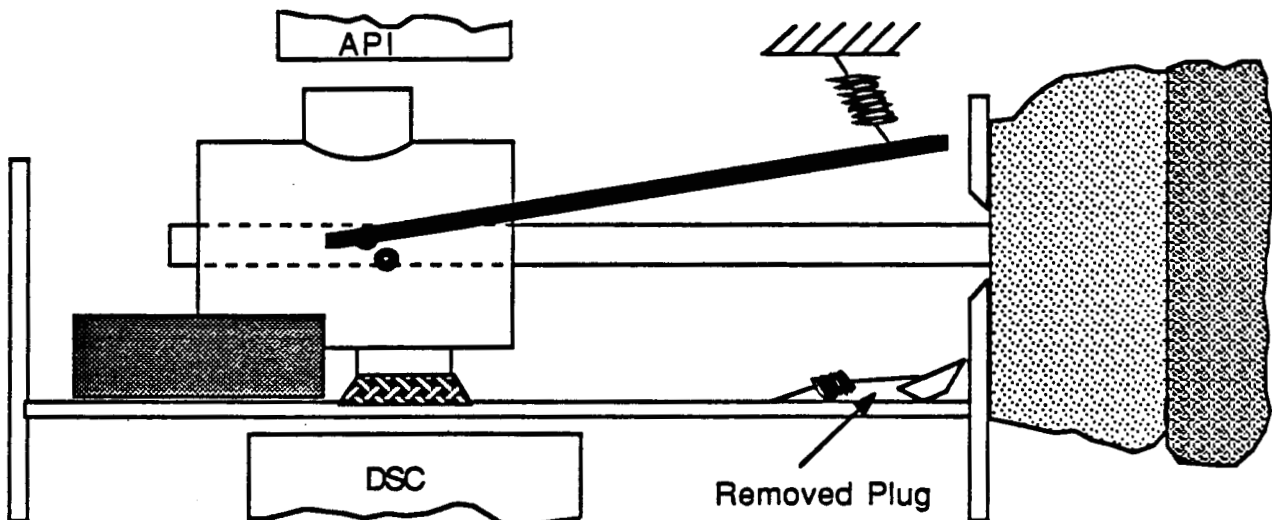
Removed Plug

Motor moves past the pivot point and allows U-Lever
to rotate. Plug is removed by plug spring.

Figure 17: Illustrated Time Sequence (2 of 5)
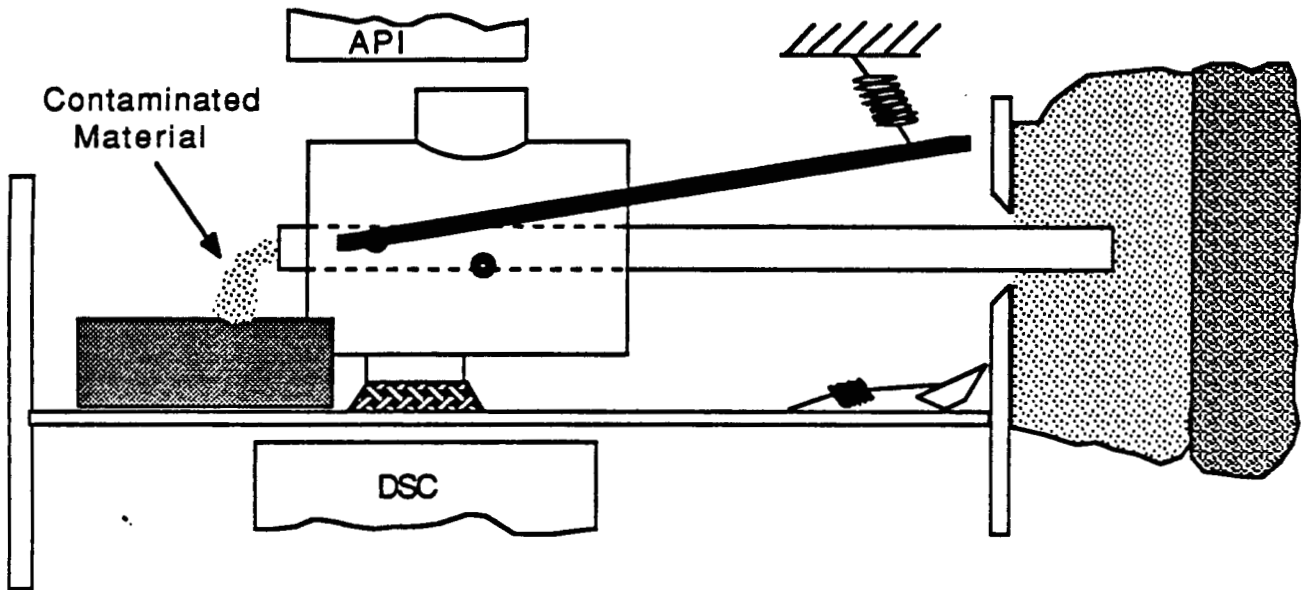
CGM moves outside the penetrator grinding material and passing it through the interior of the bit
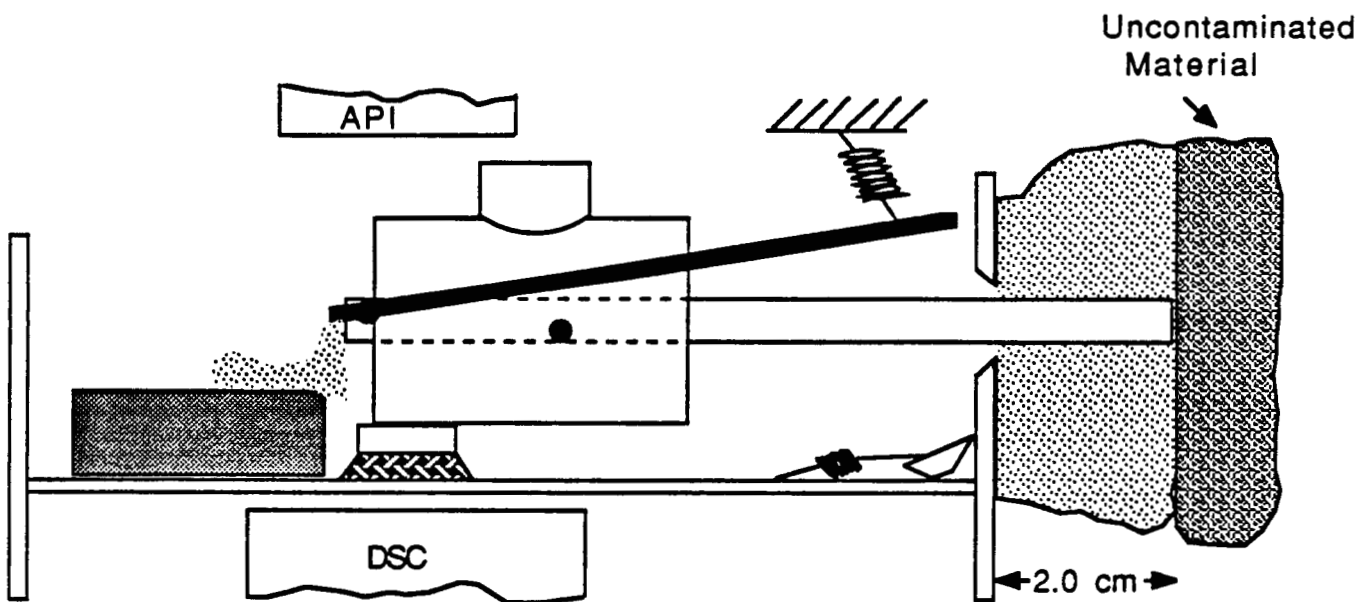
The tip of the bit encounters the desired sample

Figure 18: Illustrated Time Sequence (3 of 5)

API

Uncontaminated
Material

Initial Tray
Location

DSC
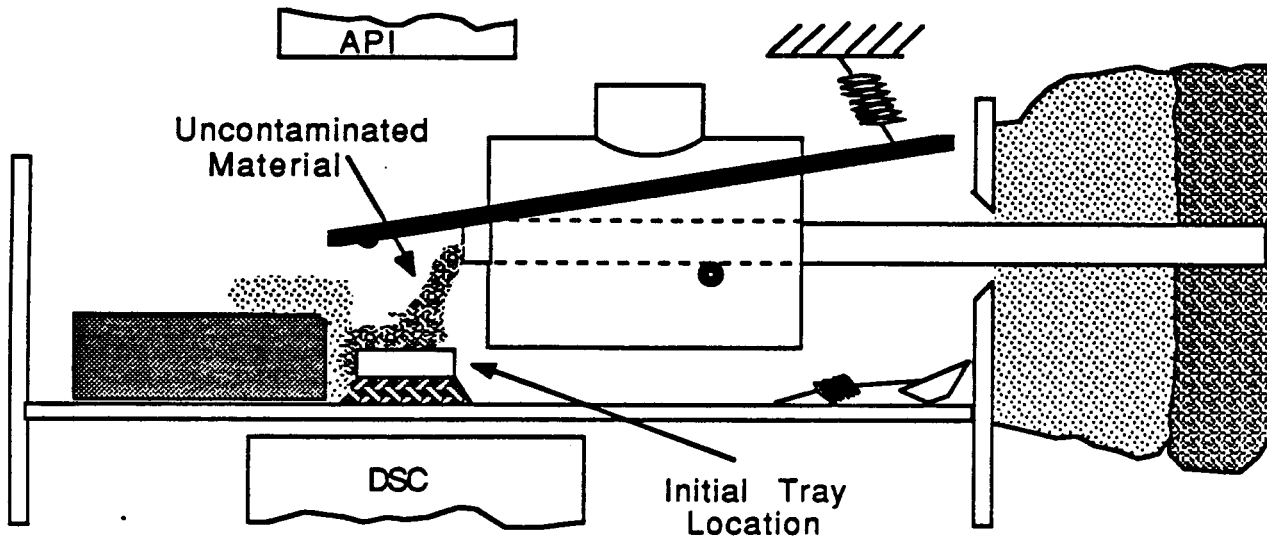
Tray is being filled with the uncontaminated sample

API

Tray

Extended
Chute

DSC
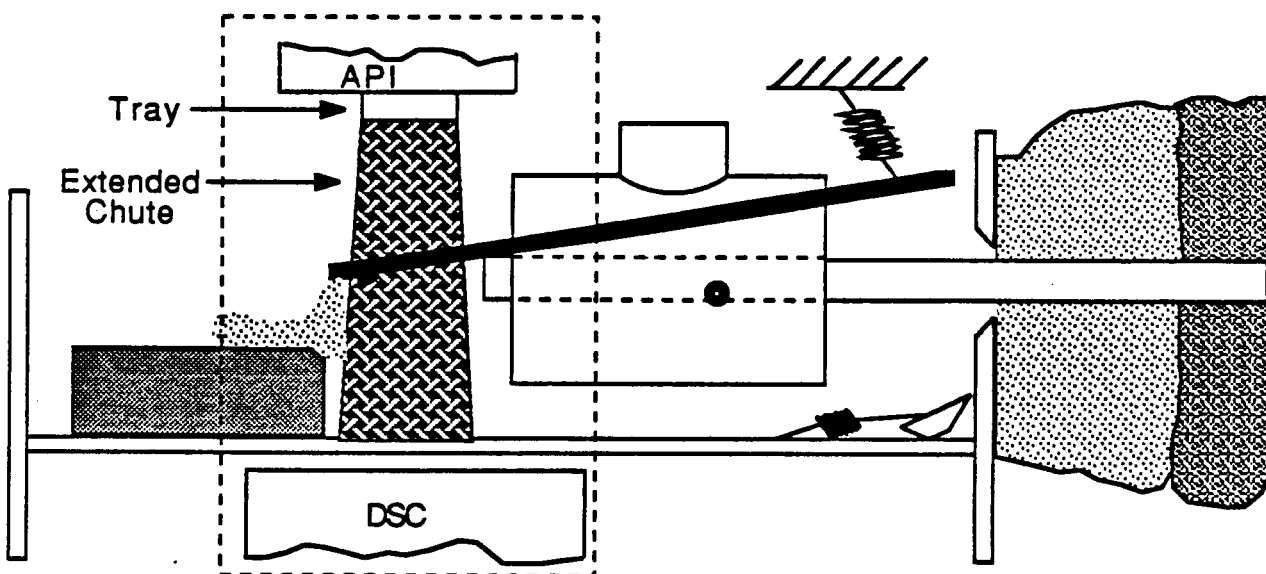
Tray contains the required amount of material. Guides on gearbox
align with slots in tray and a spring pushes the tray to API.

Figure 19: Illustrated Time Sequence (4 of 5)

API Analysis of
Sample

Sample tray is held against
API by a spring to allow for
analysis.

Trap Door

Trap door opens and sample
falls to the DSC for final
analysis.

DSC Analysis of
Sample
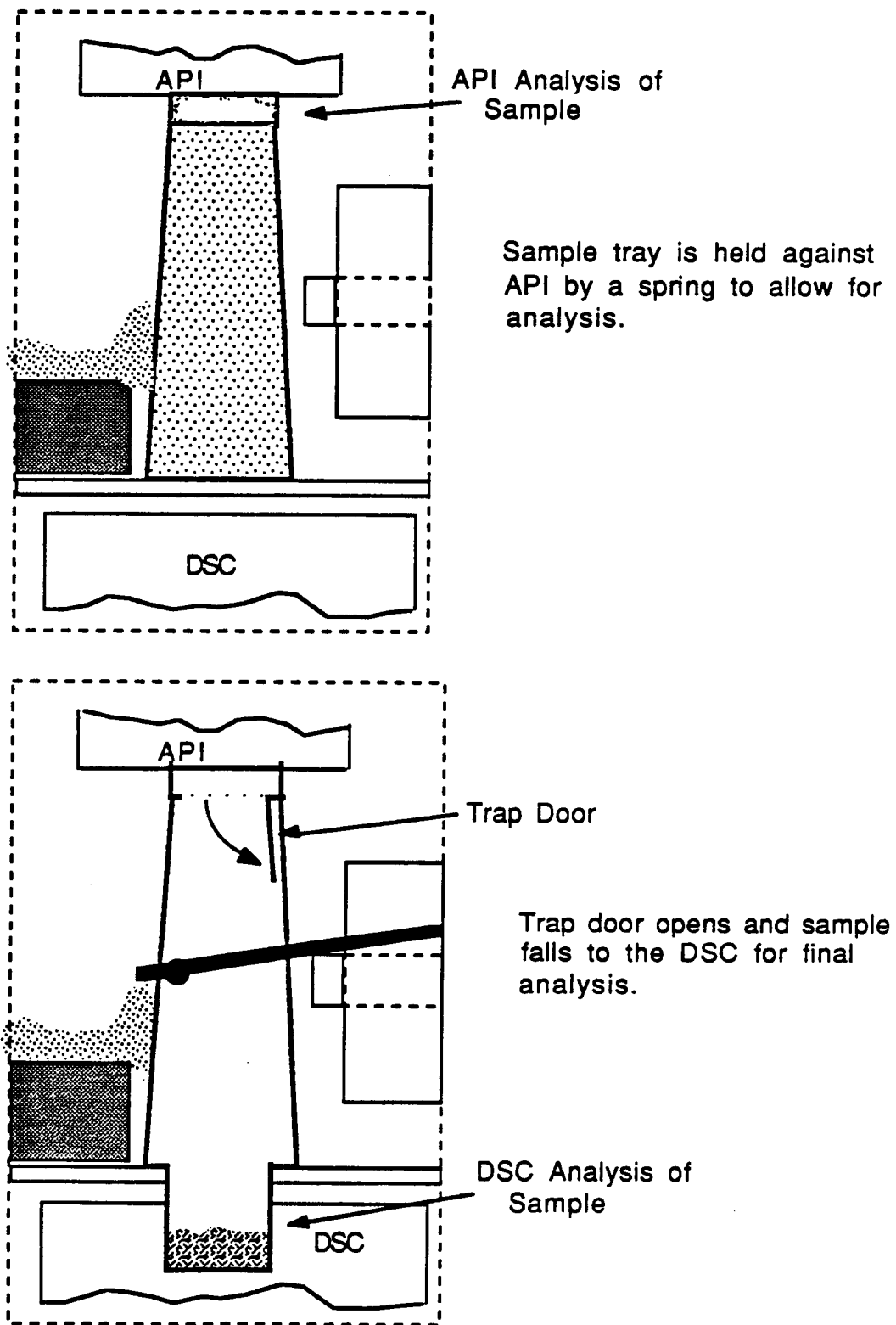
Figure 20: Illustrated Time Sequence (5 of 5)

ASSEMBLY OF PSAS COMPONENTS

- Bottom Plate - fasten plate to the interior wall using full seam weld.
- Mounting Block - weld block to bottom plate, same procedure.
- Tray - fasten spring to plate above hole to DSC, compress spring.
- Tracking Back Support and Members - slide horizontal tracking through motor
      support arms.
- Forward Support - complete all tracking connections to close rectangle.
- Plug Insertion
- U-Lever - rotate U-lever to horizontal position securing plug.
- Top Plate - fasten plate to interior wall using full seam weld.

POWER RESTRICTIONS

The design is highly mechanical in nature, the main power draw being the motor for the CGM. If problems arose in the amount of power available, we would recommend going with only one sampling system instead of two.

SIZE RESTRICTIONS

As our design stands, we have no excess room within the penetrator shell. A reduction in the available size would require one of the following:
- Replace the driving springs with a small, but power consuming linear
    actuator.
- Reconfigure the bit to incorporate telescoping action, flexibility, or
    shortening of the stored length of the bit.
- Shrink the gear box. However this would increase the rotational speeds,
    power consumption, and the heat generation.

PROBLEMS WITH THE DESIGN

After placing system in the penetrator (on earth), there is no way to pretest the system. Since the system is uni-directional, resetting the system requires complete disassembly. Also should the driver spring solenoid fail during flight the system fails.

FUTURE DESIGN OPPORTUNITIES

MANDATORY DESIGN STUDIES
The following areas need future work for the design to be complete.
- Determination of timing locks and devices
- Detail work on
  - gearbox assembly
  - motor necessary for CGM
  - sizing of components to reduce mass (eg. plate sizes, tracking member sizes, etc)
  - analysis of mass flow rates due to different motor speeds
- Durability of diamond impregnated bit

OPTIONAL DESIGN STUDIES
The following areas will enhance the overall performance of PSAS.
- Volatile containment
- Analysis of point load stresses on the suspension plates
- Prototype of core-grinder for testing of sample movement (mechanical)
- Prototype of shell/deployment for testing of plug removal, movement
- Prototype of fore/after body coupling for testing of locking mechanism and shear pins

APPENDIX

APPENDIX A
SPECIFICATIONS

1. Penetrate into substances of hardness 7 (basalt).
2. Return at least 10 mg of sample.
3. Acquisition region at least 2 cm from penetrator shell (region of unaffected soil).
4. Impact resistant to 400 g's (Earth g's).
5. Total mass less than 2 kg.
6. Contained within penetrator shell of 10.5 cm inside diameter.

APPENDIX B
SCIENTIFIC PACKAGE

Alpha Particle Instrument (API)

    The silicon detector proposed for the detection of the induced x-ray fluorescence is expected to provide highly accurate measurements of the lighter elements. From the three modes of operation for the instrument, the abundances of carbon, nitrogen, oxygen, and sulphur as well as iron and nickel should be determined to high accuracy.

Differential Scanning Calorimeter (DSC)

    This instrument is designed to take about 10mg of subsurface material and carry out a thermal study by placing the sample in a pressure type holder and increasing the sample temperature at a constant rate. A reference sample of known characteristics is placed in an identical holder and is heated at the same rate. The thermal control circuit maintains a thermal-null between the material sample and the reference material then the differential heating required to accomplish this is recorded. At three preselected temperatures for the thermal study (100,250,450 C), a valve in the sample holder is open to sample the evolved gases through the Evolved Gas Analyzer.

Evolved Gas Analyzer (EGA)

    This system is equipped with two analytical columns : a light gas column to resolve hydrogen, neon, nitrogen, oxygen, argon, carbon monoxide, methane, krypton and carbon dioxide; and a polar gas column, primarily to resolve water vapor. The EGA uses ultra-high purity helium carrier gas with metastable ionization detectors. Sampling at the three preselected temperatures will allow the unambiguous identification and measurement of such evolved species as oxygen from the "oxidative" Martian soil, carbon dioxide from thermally labile carbonates, and water of hydration from certain minerals. By comparing the results of the evolved gas analyses with exothermic and endothermic events recorded by the differential scanning calorimeter, it should be possible to obtain information on specific mineral and chemical composition of the Martian subsurface.

APPENDIX C

DEFINITION OF ACRONYMS

API : Alpha Particle Instrument

CGM : Core-Grinder Mechanism

DSC : Differential Scanning Calorimeter

EGA : Evolved Gas Analyzer

FAC : Fore/Afterbody Coupling

PIMP : Protective Impact Mounting Platform

PSAS : Penetrator Sample Acquisition System

SAD : Sample Acquisition Device

SSS : Sampling System Suspension

Appendix D-1
U-Lever Impact Stresses
Exit Plug Spring Constant

Variables

ρ	density of Ti alloy, 4460 kg/m^3
A	point load due to peg on gearbox housing
a	acceleration of impact, 400g's
B	load in y direction at pin joint
b	width of U-Lever cross-section
C	point load due to peg on tracking system
D	point load due to U-Lever cross arm mass
h	height of U-Lever cross-section
w	distributed load due to U-Lever mass

Analysis Outline

I. Determine knowns : w, D

II. $\Sigma F_y = 0$

III. $\Sigma M_B = 0$

IV. Apply Castigliano's Second Theorem with load B as the redundant

Approximate the U-Lever as
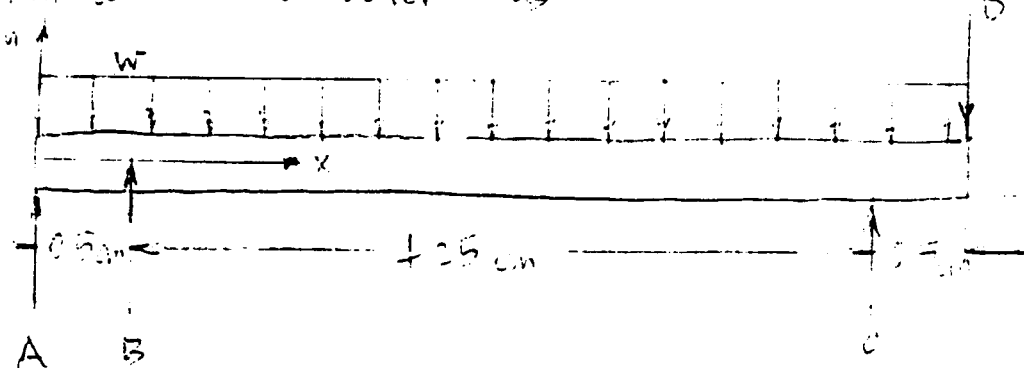
I. Distributed load w and point load D:

$$w = 2 (\rho)(bh)(a) = 3.5 \times 10^7 bh \quad [N/m]$$

$\qquad \qquad \uparrow$ symmetric U-lever

Resultant force due to w $\qquad R = wL = W(5.25 \times 10^{-2} m)$

$$R = 1.838 \times 10^6 (bh) \quad [N]$$

Point load D,

$$D = \rho\, a\, (0.0425)\, bh = 7.44 \times 10^5 bh \quad [N]$$

II. $\Sigma F_y = 0$

$$A + B + C = D + R = 2.582 \times 10^6 \, bh$$

(1) $\qquad \boxed{A + B + C = 2.582 \times 10^6 \, bh}$

III. $\Sigma M_B = 0$

$$A(0.005) + R(2.125 \times 10^{-2}) + D(0.0475) = C(0.0425)$$

(2) $\qquad \boxed{A = 8.5\, C - 1.488 \times 10^7 \, bh}$

IV. Castigliano's 2nd theorem

$$\int_0^L \frac{M}{EI} \frac{\partial M}{\partial B} \, dx = \Delta_B = 0$$

36

Moment as a function of x , $M(x)$:

$0.5 < x < 4.75$ cm

$$M(x) = -\frac{Wx^2}{2} + B(x - 0.005) + Ax$$

$4.75 < x < 5.25$ cm

$$M'(x) = -\frac{Wx^2}{2} + Ax + B(x - 0.005) + C(x - .0475)$$

So Castigliano's 2nd thm $\Rightarrow$

$$0 = \int_0^L \frac{M}{EI} \frac{\partial M}{\partial B} dx = \int_{0.005}^{0.0475} \frac{M(x)}{EI} \frac{\partial M(x)}{\partial B} dx + \int_{0.0475}^{0.0525} \frac{M'(x)}{EI} \frac{\partial M'(x)}{\partial B} dx$$

or

$$\int_{0.005}^{0.0475} M(x) \frac{\partial M(x)}{\partial B} dx = -\int_{0.0475}^{0.0525} M'(x) \frac{\partial M'(x)}{\partial B} dx$$

LHS $\Rightarrow$ $-19.15 bh + 3.012 \times 10^{-5} A + 2.56 \times 10^{-5} B$

RHS $\Rightarrow$ $-9.87 bh + 1.125 \times 10^{-5} A + 1.013 \times 10^{-5} B - 1.194 \times 10^{-5} C$

Equating LHS and RHS

(3)
$$\boxed{9.31 bh = 1.887 \times 10^{-5} A + 1.547 \times 10^{-5} B + 1.194 \times 10^{-5} C}$$

Solving eq. (1) (2) and (3) gives

$$C = 7.74 \times 10^5 bh$$

$$B = 1.01 \times 10^7 \, bh$$

$$A = -8.30 \times 10^6 \, bh$$

for a cross-section of $b = 1 \, mm$, $h = 5 \, mm$

$$A = -41.5 \, N$$
$$B = 50.5 \, N$$
$$C = 3.9 \, N$$

Shear Diagram:
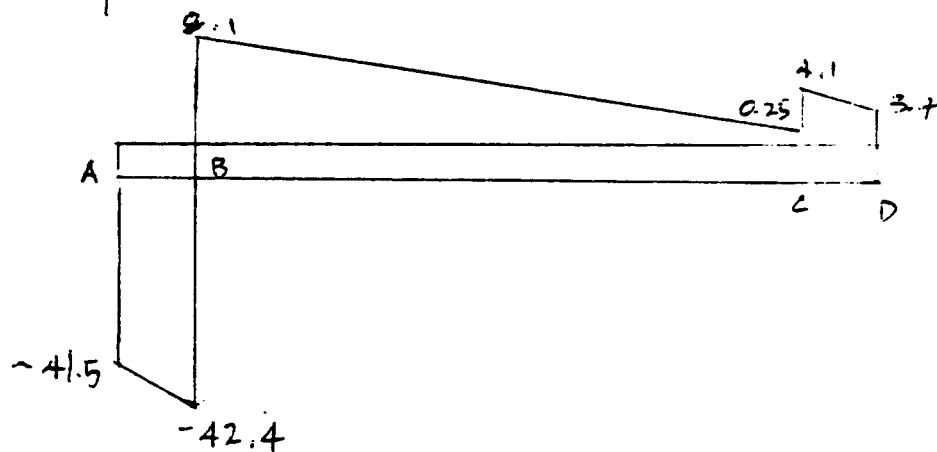
$$\tau_{max} = \frac{VQ}{It} \qquad \text{where} \qquad V_{max} = -42.5$$

$$Q = A\bar{y} = \frac{(0.005)^2}{2} (0.001)$$

$$I = \frac{1}{12} bh^3 = \frac{1}{12} (0.001)(0.005)^3$$

effective h for
point B

$$t = 0.005$$

$$\boxed{\tau_{max} = 28.7 \, MPa}$$

$$\sigma_{max} = \frac{M_{max} \, y}{I} \qquad \text{where} \qquad M_{max} \simeq 0.21 \, Nm \quad \left(\begin{array}{l}\text{from Shear} \\ \text{Diagram at B}\end{array}\right)$$

$$\boxed{\sigma_{max} \sim 238 \, MPa}$$

$$\sigma_{yield \, Ti} \sim 600 \, MPa$$

38

EXIT PLUG SPRING CONSTANT

For a removal time $t = 0.1$ sec

$$d = \frac{1}{2} a t^2 = \frac{1}{2} \left(\frac{F_{spring}}{m_{plug}} \right) t^2 = \frac{1}{2} \frac{kx}{m} t^2$$

from plug geometry

$$d = 1.0 \text{ cm}$$

assume

$$x \sim 2 \text{ cm}$$
$$t \sim 0.1 \text{ sec}$$

Mass plug = (density plug) (Volume plug)

density = 1460 kg/m³

Volume = $R_{eff}^2 \pi L$

approximate plug shape as cylindrical

$$R_{eff} = \frac{\left[1 + \frac{0.75}{2} \sin 45° + \frac{0.75}{2} \sin 60° \right]}{2}$$

$$\rightarrow .75 \text{ cm}$$

Mass plug ~ 1.922 gm

So $k_{spring} \sim \frac{2 m d}{x t^2} \sim 0.2 \left[\frac{N}{} \right]$

$$F_{spring} \sim 4 \times 10^{-3} [N]$$

Appendix D-2
Transverse Impact Loading of Core-Grinder Tracking Mechanism

Variables

a_i	impact acceleration
F_T	total transverse force
F_1	reaction load at the rear of the track
F_2	reaction load at the front of the track
M_1	reaction moment at the rear of the track
M_2	reaction moment at the front of the track
F_B	impact load at the rear of the gearbox
F_F	impact load at the front of the gearbox
r_i	distance to respective loads (i = B, F, L, U, 1, 2)
F	one-eighth of the total transverse load

Analysis Outline

I. Determine total transverse load

II. Calculate member critical radius due to shear

III. $\Sigma M_C = 0$

IV. $\Sigma M_D = 0$

V. $\Sigma F_Z = 0$

VI. Apply Castigliano's Second Theorem with load F_B as the redundant force

VII. Calculate member critical radius due to moments.

VIII. Calculate vertical member radius to combined loading

IX. Determine stabilizer arm critical area

# I. Total transverse load due to motor-gearbox mass
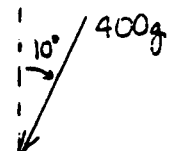
$$a_i = 400g (\sin 10°)$$
$$= \underline{69.4g} \ [m/s^2]$$

$$F_T = m_{motor} \cdot a_i$$
$$= (1.0)(69.4g) = \underline{680} \ [N]$$

II. Member critical radius due to shear (point load approximation)
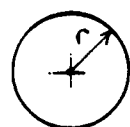
$$\tau_{yield} = \frac{VQ}{It}$$
$$= \frac{1}{6} \frac{F_T}{\pi r^2}$$

$$r = \sqrt{\frac{1}{6} \frac{F_T}{\pi \tau_y}}$$

$$= \underline{0.333} \ [mm] \leftarrow \text{conservative}$$

$$\tau_{yield} = 325 \ MPa$$
$$V = \frac{1}{8} F_T \leftarrow \text{8 members from gearbox}$$
$$I = \frac{1}{4} \pi r^4$$
$$t = 2r = D$$
$$Q = A'\bar{y} = \frac{2}{3} r^3$$
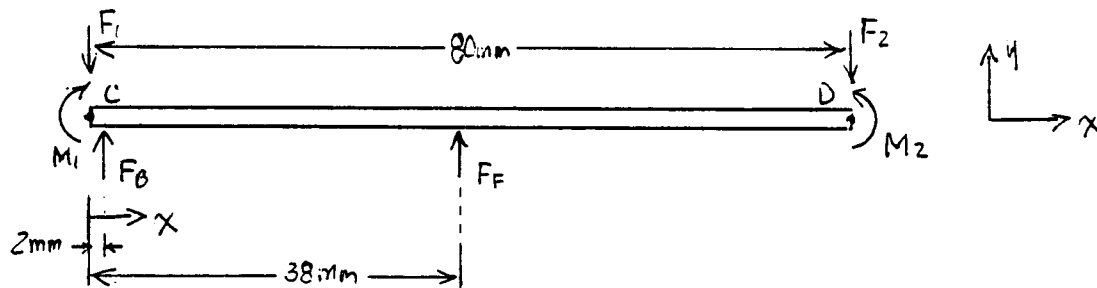
III. $\Sigma M_c = 0 \quad \curvearrowright_+$

$$M_1 = (r_B + r_F) F_F - r_2 F_2$$

$$\textcircled{1} \quad \underline{M_1 = 40,000\mu \, F_F - 80,000\mu \, F_2}$$

NOTE:
- $F_F = F_B = \frac{1}{8} F_T$
- distributed load due to weight is negligible

IV. $\Sigma M_D = 0 \quad \curvearrowright_+$

$$M_2 = (r_B + r_F) F_F - r_1 F_1$$

$$\textcircled{2} \quad \underline{M_2 = 120,000\mu \, F_F - 80,000\mu \, F_1}$$

41

$\underline{V}.\ \Sigma F_y = 0 \quad +\uparrow$

$$F_B + F_F - F_1 - F_2 = 0$$

③ ———— $\underline{\underline{2F_F - F_1 - F_2 = 0}}$

$\underline{VI}.$ Castigliano's second theorem with F_B as redundant

general form: $\int_0^L \dfrac{M}{EI} \dfrac{\partial M}{\partial P}\, dx = \Delta_P = 0$
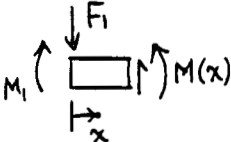
i) $M(x) = -F_1 x$

$\dfrac{\partial M}{\partial F_B} = 0$

- $r_B = 2\,mm$
- $r_F = 38\,mm$
- $L = 80\,mm$
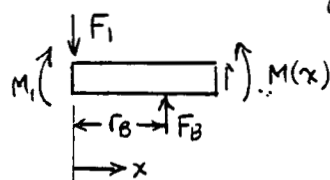
ii) $M(x) = -F_1 x + (x - r_B) F_B$

$\dfrac{\partial M}{\partial F_B} = (x - r_B)$
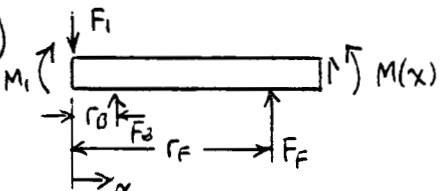
iii) $M(x) = -F_1 x + (x - r_B) F_B + (x - r_F) F_F$

$\dfrac{\partial M}{\partial F_B} = (x - r_B)$

$$0 = \int_0^L \frac{M(x)}{EI}\frac{\partial M(x)}{\partial F_B}\,dx = \underbrace{\int_0^{r_B} \frac{M(x)}{EI}\frac{\partial M(x)}{\partial F_B}\,dx}_{0} + \underbrace{\int_{r_B}^{r_F} \frac{M(x)}{EI}\frac{\partial M(x)}{\partial F_B}\,dx}_{Ⓐ} + \underbrace{\int_{r_F}^{L} \frac{M(x)}{EI}\frac{\partial M(x)}{\partial F_C}\,dx}_{Ⓑ}$$

Ⓐ $\quad -16.85\mu F_1 + 15.56\mu F_B$

Ⓑ $\quad -147.3\mu F_1 + 142.6\mu F_B + 49.99\mu F_F$

adding Ⓐ & Ⓑ

④ ———— $\underline{\underline{-164.15\mu F_1 + 158.16\mu F_B + 49.99\mu F_F = 0}}$

42

VII. Calculate stresses due to moments

from eqn ①→④ and noting that
$$\underline{\underline{F_F = F_B = \tfrac{1}{8} F_T = 85 \ [N]}}$$

$$\underline{\underline{F_1 = 107.8 \ [N]}}$$
$$\underline{\underline{F_2 = 62.2 \ [N]}}$$
$$\underline{\underline{M_1 = -1.576 \ [N\text{-}m]}}$$
$$\underline{\underline{M_2 = 1.576 \ [N\text{-}m]}}$$

On a single member:

$$\sigma_{yield} = \frac{My}{I}$$

$$r = \sqrt[3]{\frac{MI}{\tfrac{1}{4}\pi\sigma_y}}$$

$$= 1.46 \ [mm] \longleftarrow \text{minimum}$$

$$M = 1.576$$
$$I = \tfrac{1}{4}\pi r^4$$
$$y = r$$
$$\sigma_{yield} = 650 \ MPa$$

$$\therefore \ \underline{\underline{r = 1.55 \ [mm]}}$$

with Factor of Safety = $\underline{\underline{F.S. = 1.21}}$

VIII. Calculate vertical member radius

at point O:

$$\underline{F} = \tfrac{1}{8} F_T = \underline{85} \; [N]$$
$$\underline{T} = (r_F + r_B) 2F = \underline{20.4} \; [N\text{-}m]$$
$$\underline{M_y} = 2F(r_U + r_L) = \underline{5.53} \; [N\text{-}m]$$
$$\underline{V} = 4F = \underline{340} \; [N]$$
$$r_F = 42 \; [mm] \qquad\qquad r_L = 5 \; [mm]$$
$$r_B = 78 \; [mm] \qquad\qquad r_U = 27.5 \; [mm]$$
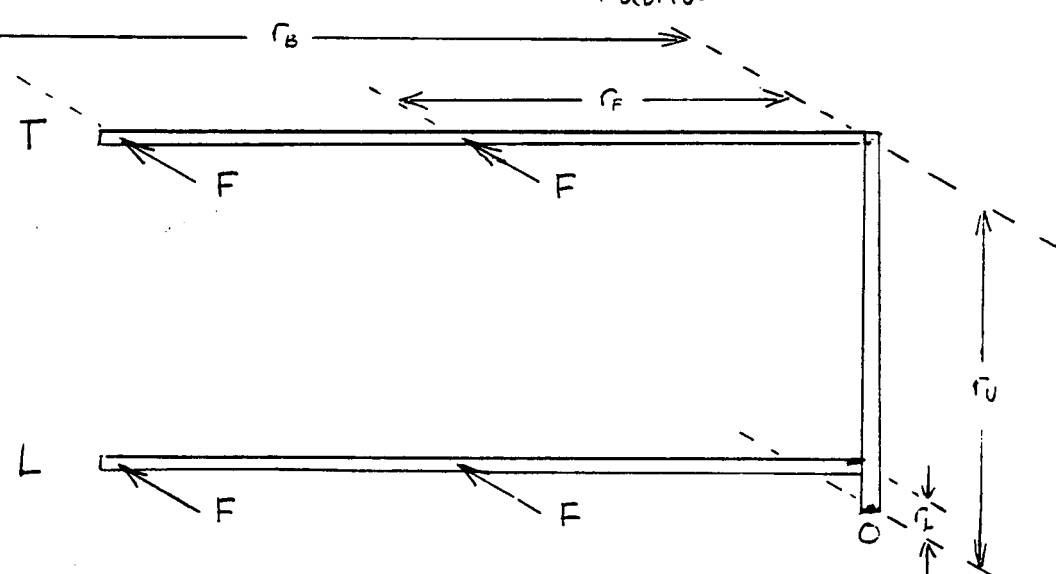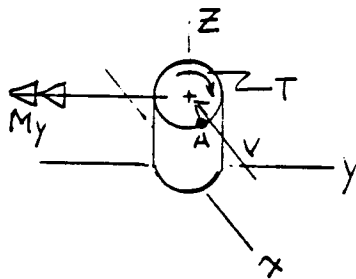
$$\tau_{zy} = \frac{Tc}{J} = \frac{T}{\tfrac{1}{2}\pi c^3}$$
$$= \underline{300} \; [MPa]$$

$$C = \underline{3.5} \; [mm]$$

$$\underline{\sigma_z} = \frac{Mc}{I} = \frac{M}{\tfrac{1}{4}\pi c^3} = \underline{164.2} \; [MPa]$$

$$\underline{\sigma_{MAX}} = \frac{\sigma_z + \cancel{\sigma_y}^{\,0}}{2} + \sqrt{\left(\frac{\sigma_z - \cancel{\sigma_y}^{\,0}}{2}\right)^2 + \tau_{zy}^2}$$
$$= \underline{396} \; [MPa]$$

$$\underline{\tau_{MAX}} = \sqrt{\left(\frac{\sigma_z - \sigma_y}{2}\right)^2 + \tau_{zy}^2}$$
$$= \underline{314} \; [MPa]$$

$$\sigma_{MAX} \,\&\, \tau_{MAX} < \sigma_{yield}$$
$$\therefore \; ok$$

IX. Determine stablizer arm critical area

$$\sigma = \frac{F}{A} \;\rightarrow\; A \geq \frac{F}{\sigma_y} = \underline{1.31 \times 10^{-7}} \; [m^2]$$

$$\underline{b = h = 1.5} \; [mm]$$
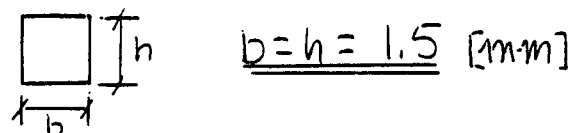
$$P_{cr} = \frac{\pi^2 EI}{Le}$$

$$Le = \frac{\pi^2 EI}{P_{cr}}$$
$$= \underline{22.5} \; [mm]$$

$$Le = L$$
$$\underline{E = 115} \; [GPa]$$
$$I = \tfrac{1}{3} b h^3 = 1.688 \times 10^{-12} \; [m^4]$$

$$\therefore \; arm \; must \; be \; less \; than$$
$$22.5 \cdot mm \; in \; length \; to \; avoid$$
$$buckling$$

44

Drill Bit Calculations

Variables

$\dot{z}_{tot}$ velocity of dirt particle with respect to tray

$\dot{z}_{rel}$ velocity of dirt particle with respect to inside of bit

$\dot{z}_{bit}$ forward velocity of bit into soil

z direction along bit axis

ω angular velocity

γ pitch angle of internal threads

H hypotenuse of thread

D effective diameter of bit

l distance between threads

L total length of inner bit

c damping coefficient

F back pressure drilling force (average force = 35 pounds)

Analysis Outline

I. Soil return rate

II. Pitch angle

III. Velocity of sample as it exits bit

IV. Drill Bit

V. Amount of sample obtained
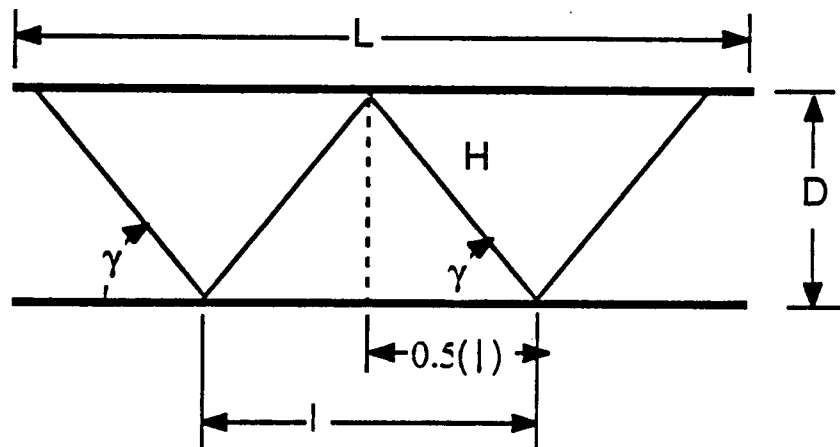
- <u>SOIL RETURN RATE</u>:
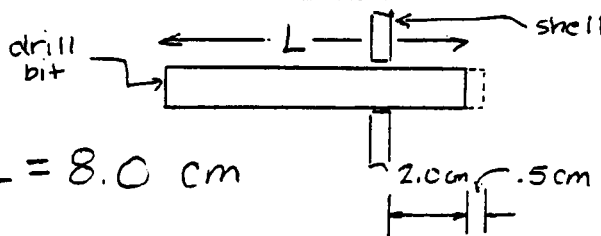
- $L = 8.0$ cm

ORIGINAL PAGE IS
OF POOR QUALITY

<u>NEEDED</u>: At 2.5 cm, the material contacted at 2.0 cm
  is falling into the tray
  ie. drill moves out 0.5 cm while dirt moves in 8.0 cm

$\Rightarrow \dfrac{8.0 \text{ cm}}{0.5 \text{ cm}} = 16/1$ = ratio of distances and relative velocities

define: velocity of bit $= 1 \cdot \forall = \dot{z}_{bit}$
        velocity of dirt $= 16 \forall = \dot{z}_{rel}$

Drilling speeds:

- $\omega|_{outer\ bit} = 360$ rpm   : determined from drilling tests

- Gear ratio $= \dfrac{outer\ bit}{inner\ bit} = 1/4 \Rightarrow \omega)_{inner\ bit} = 360(4) = 1440$ rpm $= \underline{24\ r/s}$

- Threads:
  $\ell = \dfrac{\text{Distance soil moves}}{\text{revolution}}$ = distance between threads

  Assuming that the soil particle does not slip and moves the distance between threads for a single turn of the bit

  $\dot{z}_{rel} = (2H\cos\gamma)\omega(2\pi)$

- Damping factor: $m\cancel{\ddot{z}}^{0} + c\dot{z} + \cancel{k\dot{z}}^{0} = F$; NO ACCELERATION
                                                                NO SPRINGS

  $\Rightarrow c\dot{z} = F$

  OR $\dot{z}_{bit} = \dfrac{F}{c}$ maximum forward velocity of bit

Velocity ratio:

- $\dfrac{\dot{z}_{rel}}{\dot{z}_{bit}} = \dfrac{2H\cos\gamma\ \omega(2\pi)}{F/c} = \dfrac{2H\left[\frac{\ell}{2H}\right]\omega 2\pi}{F/c} = \dfrac{\ell\omega 2\pi}{F/c} = \dfrac{\dot{z}_{rel}}{\dot{z}_{bit}}$

therefore

- $\ell = \left(\dfrac{\dot{z}_{rel}}{\dot{z}_{bit}}\right)\dfrac{F}{2\pi c\omega}$

46

- <u>SOIL RETURN RATE</u>

conversion $\frac{lb \cdot s}{in} \rightarrow \frac{N \cdot s}{mm}$

- $\left[\frac{lb \cdot s}{in}\right]\left(\frac{4.448N}{lb}\right)\left(\frac{1\ in}{25.4\ mm}\right) = \underline{0.1751\ \frac{N \cdot s}{mm}}$

Assume centripetal force keeps dirt to outside of bit at all times.

Calculation of l :

$l = \frac{\dot{z}_{bit}}{\dot{z}_{rel}}\left(\frac{F}{2\pi c \omega}\right)$; $F)_{AVE} = \frac{50 + 15}{2}$ 32.5 lb

$\therefore\ l = \left(\frac{16}{1}\right)\frac{32.5\ lb}{c\ (24\ rps)(2\pi\ ^{rad}/_r)}$

$l = \dfrac{3.45}{c}$

variation of c with l and γ

$c\ \frac{N \cdot s}{mm}$	$l\ mm$	γ	
0.0431	80 (length of bit)	γ max	$\Rightarrow$ one thread from end to end (one extreme)
∞	0	$0°$	$\Rightarrow$ infinitely many threads
0.6271	5.50	$45°$	$\Rightarrow$ optimizes backwards force due to threads and outward force.

- choose $l = 5.50\ mm$; $D = 2.75\ mm$

$c = 0.6271\ \frac{N \cdot s}{mm} = 3.58\ \frac{lb \cdot s}{in}$

- $\gamma = \cos^{-1}\left(\frac{l}{2H}\right) = \cos^{-1}\left[\frac{l}{2[D^2 + (l/2)^2]^{1/2}}\right]$

$\underline{\gamma = 45°}$ pitch angle

- ## DRILL

  pitch angle = 45°

  distance between threads = 5.50 mm

- ## Velocity of Sample Exiting Bit

  $$V_{TOT} = V_{rel} - V_{BIT}$$

  $$= 2H \cos \gamma \omega - F/c$$

  $$= 2H \frac{l}{2H} \omega - F/c$$

  $$= l\omega - F/c$$

  $$= (5.50 \text{ mm})(24 \text{ r/s})(2\pi \text{ rad/r}) - (32.50 \text{ lb})/3.58 \frac{lb \cdot s}{in}$$

  $$= 829.38 \text{ mm/s} - 9.0782 \frac{in}{s} \left(\frac{25.4 \text{ mm}}{in} \right)$$

  $$\underline{V_{TOT} = 598 \text{ mm/s} = 1.364 \text{ mi/hr}} \qquad \text{Velocity Sample exits bit}$$

  <u>Note</u>: This velocity represents the bit moving into a substance of negligible resistance (ie powdered chalk) at the maximum forward velocity allowed by the dashpot. It also assumes "no slip" between the sample and the internal threads. Therefore, the actual exit speed of the sample will be much less for real conditions.

DRILL BIT

drill motion
0.5 cm (forward)

drill bit

tray

← K →

←0.5 cm→
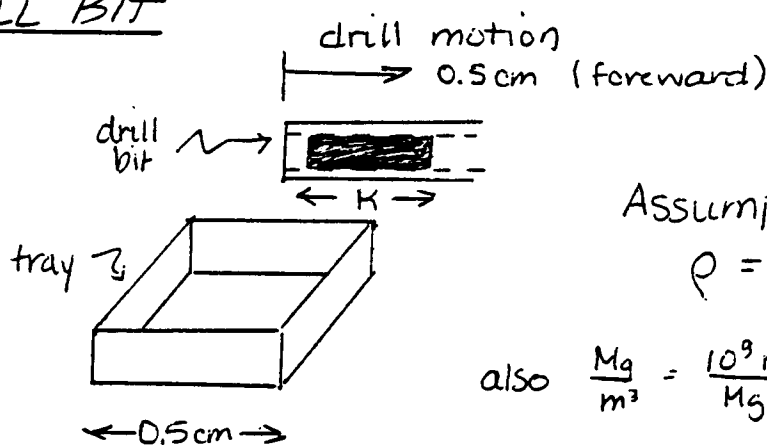
Assumptions:

$\rho = 1.5 \frac{Mg}{m^3}$ chalk → lightest substance to encounter

also $\frac{Mg}{m^3} = \frac{10^9 \, mg}{Mg} \left(\frac{m}{1000 \, mm}\right)^3 = mg/mm^3$

Sample mass needed: mass = 10 mg

Volume: $\forall = \frac{m}{\rho}$

also $\forall = \frac{\pi}{4} D^2 K$

$\left. \right\}$ $\frac{m}{\rho} = \frac{\pi}{4} D^2 K \Rightarrow K = \frac{4m}{\rho \pi D^2}$

$K = \frac{4(10 \, mg)}{\left(1.5 \frac{mg}{mm^3}\right)(\pi)(2.75 \, mm)^2} = 1.122 \, mm$

$\underline{K = 1.122 \, mm}$

INNER BIT
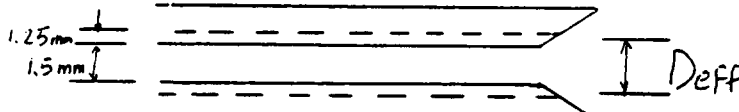
1.25 mm
1.5 mm

D_{eff}

$D_{eff} = 1.5 \, mm + 2\left(\frac{1.25 \, mm}{2}\right)$

$\underline{D_{eff} = 2.75 \, mm}$

K = 1.122 mm   corresponds to the length of the sample tube needed to get 10 mg.

Actual Amount of Sample Obtained

$m = \rho \forall = \rho \frac{\pi}{4} (D_{eff})^2 K$

$= \left(1.5 \frac{mg}{mm^3}\right) \frac{\pi}{4} (2.75 \, mm)^2 (0.5 \, cm)$

$\underline{m = 44.55 \, mg \text{ of sample}}$ ⇒ 4.4 times more sample than needed

• Therefore, we have a large margin of safety for the amount of material to be passed through the bit into the tray. This is necessary since: (1) we assumed the ideal case of the bit full of sample (2) this accounts for sticking, compressibility.

- DRILL BIT

Titanium Alloy : $\sigma_y = 126$ ksi $= 868.8$ MPa

- Moment on Inner Bit : $\tau = \dfrac{Mc}{I} \cong 0.8$ MPa

Deflection of bit due to weight of soil

- $V = \dfrac{-qL^4}{8EI} = 1.16 \ \mu m$

Normal Force $\sigma_N = \dfrac{F}{A} = 5.7$ MPa

- Buckling load : $P_{CR} = \dfrac{\pi^2 EI}{L_e^2}$

$P_{CR} = 37.54$ kN

- Torque $T = \dfrac{\tau J}{c}$

$T = 13.43 \ N \cdot m$

50

Variables

$\bar{D}$	average diameter
P	load
FL	full length of spring
F	deflection
f	deflection/coil
OD	outer diameter
ID	inner diameter
S	stress
N	number of active coils
TC	total coils
SH	solod height or compressed height
I	average spring index
K	curvature correction factor
S_T	total stress
G	shear modulus
R	spring rate
d	wire diameter
S_S	solid stress
$(S_S)_T$	total solid stress

Analysis Outline

I. Sample Placement Tray

    A. Force required to lift tray and sample

    B. Spring Calculation

II. Driving Spring Calculation

Reference for figures mentioned in calculation : <u>Spring Designer's Handbook</u> by Harold Carlson.

I Sample Placement Tray

A. Force required to lift tray

Total mass $M = m(sample) + m(tray)$

$m(tray) = \forall \rho$; ρ (titanium)

$m(tray) = 0.00129$ kg

$m(sample) = 0.00001$ kg

$M = 0.00130$ kg

Force $= [m(tray) + m(sample)] \times [$gravitational accel. on Mars$]$

$= (.00130 \, kg)(\frac{1}{3} 9.81 \, m/s^2)$

force $= 0.00425$ N

B. Spring Calculations

• Conical spring $FL = 7cm = 2.75"$

• At compressed height of $L = 6cm = 2.36"$

$P = 0.00425$ N

INNER DIAMETER (TOP) $ID = .707$ cm
OUTER DIAMETER (BASE) $OD = 1.5$ cm

AVERAGE DIAMETER $\bar{D} = \dfrac{(.707 + .05) + 1.5}{2} = 1.1285$ cm

$= .444"$

$P(solid \, height) = \dfrac{P}{f} \times FL = 0.02975$ N

$= 0.13$ lb

FROM FIG (115) with $\left.\begin{array}{l} \bar{OD} = .4375 \\ P = 1.006 \\ f = 0.220" \end{array}\right\}$ $d = 0.022"$

Percent Method : find percent of actual load to P from Fig

$\% = \dfrac{0.13}{1.006} \times 100\% = 13\%$

Stress : $S = \% (100000) = 13000$

deflection/coil $f = \% (f - \text{fig } 115)$ for spring brass
mult by 2.24

$f = (.13)(.220)(2.24) = 0.064"$

Number of Active Coils $N = \dfrac{f}{f} = 6.15 \cong 7$

Total Coils $TC = N + 2 = 9$

Checking stresses

Solid Stress : $S_s = \dfrac{S}{F}(FL - d) = \dfrac{13000}{.3937}(2.75 - .022) = 90078 \text{ p.}$

Average Spring Index : $I = \dfrac{OD}{d} - 1 = 19.2$

Curvature Correction factor : Fig (114) ; $I = 19.2 \Rightarrow K = 1.06$

Total Stress : $S_T = K \cdot S = 13780$

Recommended Design Stresses fig (100)

light service , Brass wire , ASTM B·134 , 0.02" wire dia

$S_D = 52,000 \text{ psi}$

∴ will not take permanent set.

Spring Rate : $R = \dfrac{G \, d^4}{8 D^3 N}$

$G = 5\,000\,000 \text{ psi}$

$R = 0,127 \text{ }^{lb}/in$

∴ Final Results

Brass wire ASTM B 134

$d = 0.02" = .05 \text{ cm}$

With $N = 9$ coils ; ends closed and ground

II Driving Springs Calculations

2 springs; calculated for one spring and half load required.

$FL = 9 cm = 3.54"$

At compressed height of $L = 4cm = 1.57"$; $F = 5cm = 1.97"$

$$P = 25 \text{ lb}$$

Again by Fig. (115)

$$\left.\begin{array}{l} P = 28.7 \text{ lb} \\ f = 0.1724" \\ OD = 0.7813" \end{array}\right\} d = 0.08"$$

By the Percent Method

$$\% = \frac{25}{28.7} \times 100\% = 87.1\%$$

Stress: $S = \%(100000) = 87100 \text{ psi}$

deflection/coil: $= \% f = 0.150 \text{ "/coil}$

Number of Active coils $N = \frac{F}{f} = \frac{1.97}{0.150} = 13$

Total Coils $TC = N + 2 = 15$

Solid Height $SH = TC(d) = 1.2" = 3.05 \text{ cm}$

total deflection $F' = FL - SH = 2.34"$

Solid Stress: $S_s = \frac{S}{F} F' = 103460 \text{ psi}$

Average Spring Index: $I = \frac{OD}{d} - 1 = 8.7$

Curvature Correction factor (Fig 114) $k = 1.17$

Total Stress: $S_T = S \cdot k = 101907 \text{ psi}$

Total Solid Stress $(S_s)_T = S_s \cdot k = 121050 \text{ psi}$

Using ASTM A229 (MB Grade) - Oil Tempered Steel Wire
— will not take permanent set

Spring Rate : G = 11501500 psi

$$R = \frac{Gd^4}{8D^3N} \quad ; \quad R = 9.5 \ \text{lb/in}$$

$$P(L = 7\,cm) = (.787)(9.5\ \text{lb/in}) = 7.5\ \#$$

2 springs $P(\text{3 cm into soil}) = 15\ \text{lb}$

∴ Final Results

    Oil Tempered Steel Wire   ASTM A 229 (MB grade)

      $d = 0.08'' = 0.2\ cm$

    With N = 15 coils ends closed and ground

    S.H. = 3.05 cm

Appendix D-7
Suspension Calculations

Variables

υ	Poisson's ratio
W	annular line load
R	outside radius of plate
r	radius of hole in plate
r_o	distance from center to load w
a	acceleration
m	mass
g	gravity
τ	shear stress
c_1	plate constant dependent on ratio R/r
c_4	plate constant dependent on ratio R/r
L_6	Load constants dependent on ratio R/r_o
L_3	"
L_{11}	"
L_{14}	"
y_b	vertical deflection of plate
q	load per unit area
D	plate constant

Analysis Outline

I. Deflections of Flat Plates

II. Strength of material in shear

III. Strength of weld in shear

I. FLAT PLATE THEORY

A. ASSUMPTIONS

1. THE PLATE IS FLAT, OF UNIFORM THICKNESS AND OF HOMOGENEOUS ISOTROPIC MATERIAL.

2. THE THICKNESS IS NOT MORE THAN ONE QUARTER OF THE LEAST TRANSVERSE DIMENSION, AND THE MAXIMUM DEFLECTION IS NOT MORE THAN ABOUT ONE HALF THE THICKNESS.

3. ALL FORCES - LOADS AND REACTIONS ARE NORMAL TO THE PLANE OF THE PLATE.

4. THE PLATE IS NOT STRESSED BEYOND THE ELASTIC LIMIT

B. EQUATIONS

TWO DIFFERENT CASES WERE USED TO CHECK THE VALIDITY. ONE CASE BEING AN ANNULAR PLATE WITH A UNIFORM ANNULAR LINE LOAD OF w AT A RADIUS r_0. THE OTHER BEING AN ANNULAR PLATE WITH A DISTRIBUTED LOAD OF q OVER THE PORTION FROM r_0 TO R.

1. ANNULAR PLATE WITH A UNIFORM ANNULAR LINE LOAD OF w AT A RADIUS r_0, OUTER EDGE FIXED INNER FREE.

$$y_b = -\frac{wR^3}{D}\left(\frac{C_1 L_6}{C_4} - L_3\right)$$

$$C_1 = \frac{1+v}{2}\frac{r}{R}\ln\frac{R}{r} + \frac{1-v}{4}\left(\frac{R}{r} - \frac{r}{R}\right)$$
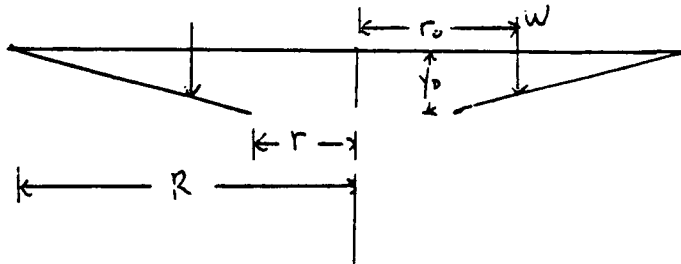
$$L_6 = \frac{r_0}{4R}\left[\left(\frac{r_0}{a}\right)^2 - 1 + 2\ln\frac{R}{r_0}\right]$$

$$C_4 = \tfrac{1}{2}\left[(1+v)\frac{r}{R} + (1-v)\frac{R}{r}\right]$$

$$L_3 = \frac{r_0}{4R}\left\{\left[\left(\frac{r_0}{R}\right)^2 + 1\right]\ln\frac{R}{r_0} + \left(\frac{r_0}{R}\right)^2 - 1\right\}$$

$$R = .0525\,m \qquad W = 3924N$$
$$r = .005\,m$$
$$r_0 = .0225\,m$$
$$v = .3$$

$$y_b = -1.368 \times 10^{-5}\,m$$

2. ANNULAR PLATE WITH A UNIFORMLY DISTRIBUTED LOAD q OVER THE PORTION FROM r_0 TO R.
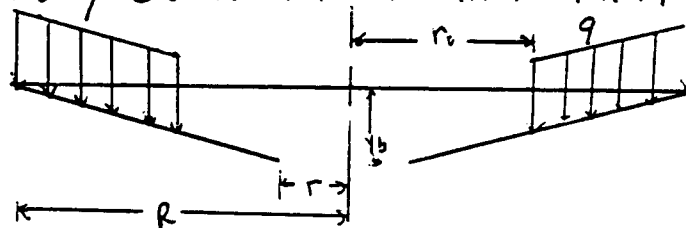
$$y_b = -\frac{q R^4}{D}\left(\frac{C_1 L_{14}}{C_4} - L_{11}\right)$$

$$C_1 = \frac{1+v}{2}\frac{r}{R}\ln\frac{R}{r} + \frac{1-v}{4}\left(\frac{R}{r} - \frac{r}{R}\right)$$

$$L_{14} = \frac{1}{16}\left[1 - \left(\frac{r_0}{R}\right)^4 - 4\left(\frac{r_0}{R}\right)^2 \ln\frac{R}{r_0}\right]$$

$$C_4 = \frac{1}{2}\left[(1+v)\frac{r}{R} + (1-v)\frac{R}{r}\right]$$

$$L_{11} = \frac{1}{64}\left\{1 + 4\left(\frac{r_0}{R}\right)^2 - 5\left(\frac{r_0}{R}\right)^4 - 4\left(\frac{r_0}{R}\right)^2\left[2 + \left(\frac{r_0}{R}\right)^2\right]\ln\frac{R}{r_0}\right\}$$

$$R = .0525\,m \qquad q = 4.53169 \times 10^5\,N/m^2$$
$$r = .005\,m$$
$$r_0 = .0225$$
$$v = .3$$

$$y_b = -3.154 \times 10^{-5}\,m$$

C. CONCLUSIONS

AS SEEN BOTH DEFLECTIONS CAN BE CONSIDERED NEGLIGIBLE AND WILL NOT AFFECT THE STABILITY OF THE PLATE. ANY DEFLECTION SHOULD DISSIPATE AFTER A SHORT TIME DUE TO THE ELASTICITY OF THE MATERIAL.

THIS THEORY ASSUMES A CIRCULAR PLATE WITH A

CENTERED HOLE. THE DESIGN ACTUALLY HAS A
NONCENTERED HOLE. THE THEORY ALSO DOESN'T
TAKE INTO ACCOUNT RANDOMLY PLACED POINT LOADS.
THESE DIFFERENCES WON'T SIGNIFICANTLY ALTER THE
OUTPUT BUT SHOULD BE LOOKED AT CLOSER.

II FORCES ON PLATE

AT IMPACT THE PENETRATOR WILL BE SUBJECTED
TO A 400 g FORCE.

$$F = m \cdot a$$

$$M = 1.0 \, Kg$$
$$a = 400 \, (9.81 \, m/s)$$
$$F = 3924 N$$

$$q = \frac{F}{A} = 4.53169 \times 10^5 \, N/m^2$$

III STRENGTH OF MATERIAL IN SHEAR

Ti-5AL-2.5SN WAS CHOSEN FOR THE PLATE MATERIAL BECAUSE
OF ITS HIGH STRENGTH AND LOW WEIGHT. IT WAS ALSO
CHOSEN BECAUSE THE SHELL IS MADE OF THE SAME
MATERIAL AND THIS WILL ELIMINATE THE FORCES THAT
MIGHT BE CAUSED BY A DIFFERENTIAL CONTRACTION
BETWEEN THE PLATE AND SHELL.

$$\tau = F/A$$

$$A = \theta \cdot r \cdot t = 1.65 \times 10^{-5} \, m$$

$$\tau = 238 \, mpa$$

$$\tau_{max} = \frac{3}{2} \tau = 357 \, mpa$$

$$\tau_{y.s.} \text{ FOR MATERIAL} = 517 \, MPA$$

IV STRENGTH OF WELD IN SHEAR

A. ASSUMPTIONS.

THE NUMBERS USED IN THIS SECTION COME FROM TESTS DONE ON $Ti-7Al-2Cb-1Ta$ PLATES. IT IS ASSUMED THESE NUMBERS WILL CLOSELY REFLECT THE NUMBERS IF $Ti-5Al-2.5Sn$ WAS USED.

$\tau_{y.s.}$ OF WELD $= 510$ MPA

Forebody/Afterbody Coupling Calculations

Variables

ρ	average density of Martian atmosphere to an altitude of 10km, kg/m^3
D	drag force of parachute, N
V	free stream velocity of wind during descent, m/s
C_d	coefficient of drag
A	projected area of parachute, m^2
r	radius of parachute, m
p	atmospheric pressure, Pa
R	universal gas constant
T	absolute temperature, K
c	speed of sound in Martian atmosphere, m/s
c_v	constant volume specific heat
c_p	constant pressure specific heat
μ	kinematic viscosity, poise
Re	Reynolds number, dimensionless
F(design)	design load to shear the pins, N
g(design)	design load to shear the pins, g's
g(drag)	acceleration due to parachute, g's
g(nose)	axial acceleration due to impact of penetrator nose = 400g's
m	mass of forebody = 15kg
P	maximum force to shear the pins, N
L	circumference of the pins, m
s	resistance to shearing, Pa
t	thickness of the pin, m
F_y	axial force due to impact of nose, N
F_x	transverse force due to lateral velocity at impact, m/s
V_y	axial velocity at impact = 100m/s
V_x	maximum lateral velocity at impact, m/s
M	moment on inner cylinder due to lateral impact velocity, N m
F_m	equivalent force on inner cylinder due to moment M, N
F.S.	factor of safety
I	moment of inertia, m^4
r_o	outside radius of inner cylinder = 5.25 cm
r_i	inside radius of inner cylinder, m
d	thickness of inner cylinder, m
δ	deflection of locking beam, m
P_{pin}	load to deflect the locking beam, N
P_{cr}	load to buckle locking beam, N
T_{cr}	torque to buckle locking beam, N m

Analysis Outline

I. Discussion of loads encountered

II. Estimation of parachute load
    A. model
    B. solve drag equation

III. Determination of design load to shear the pins

IV. Design of shear pins

V. Thickness of inner cylinder

VI. Design of locking beams
    A. beam dimensions
    B. torque for beam failure

I. Discussion of loads encountered

The 400g deceleration caused by the impact of the tip of the penetrator creates a compressive, axial load between the forebody and the after body. This load is carried through the outer shell and does not affect the shear pins.

The 1500g to 2000g deceleration induced by the impact of the tail section causes a tensile, axial load which will shear off the pins.

The deployment of the parachute during descent through the Martian atmosphere will also cause a tensile, axial load. The shear pins must resist the parachute load.

II. Estimation of parachute load
A. model

$$D = \frac{1}{2} \rho V^2 C_d A \qquad \left(\begin{array}{c}\text{drag} \\ \text{equation}\end{array}\right.$$
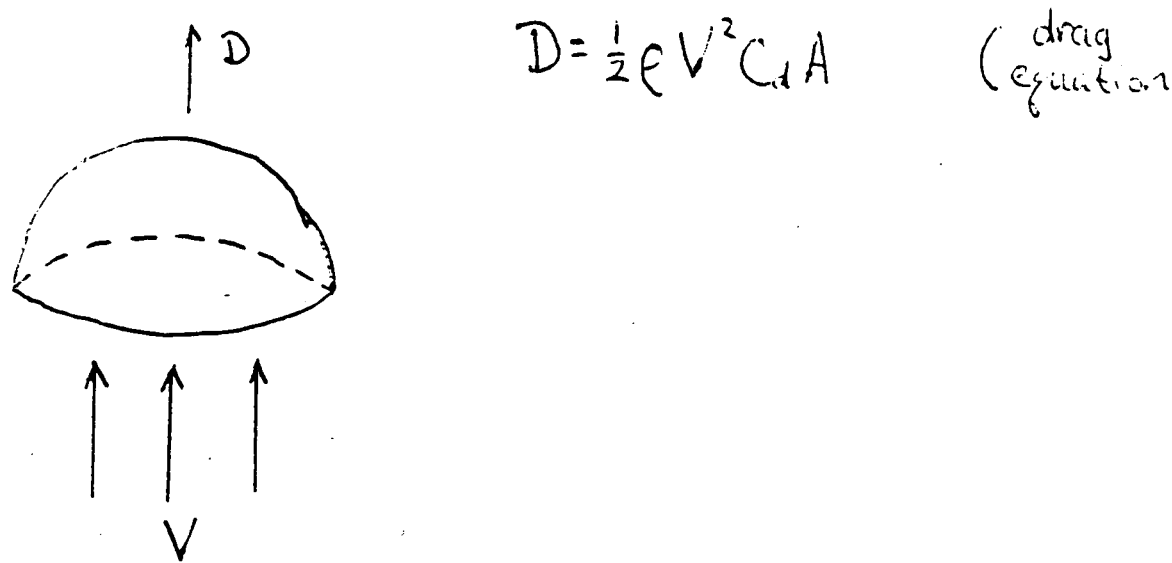
B. solve drag equation

Since the Martian atmosphere is 95% CO_2, ideal gas behavior is assumed.

$$\Rightarrow \rho = \frac{P}{RT}$$

63

The penetrator parachute is deployed at an altitude of 10 km.
It is known that pressure varies linearly from the
surface of Mars to an altitude of 200 km, where

$$p(surface) = 7 \, mbar$$

$$p(200 \, km) = 10^{-9} \, mbar$$

$$\therefore p(10 \, km) = 6.65 \, mbar$$

$$p = p(average) = \frac{p(surface) + p(10 \, km)}{2} = 6.83 \, mbar$$

$$T = 230 \, K$$

$$R = 188.9 \quad J/kg \cdot K$$

plug in to $\rho = \dfrac{p(average)}{RT}$

$$\Rightarrow \rho = 0.0153 \, \frac{kg}{m^3}$$

It is known that $V = 0.6 \, c$

$$c = \sqrt{kRT} \quad \text{where} \quad k = \frac{C_p}{C_v} = 1.29$$

assuming the atmosphere is pure CO_2

$$\Rightarrow V = 133 \, \frac{m}{s} \qquad\qquad \Rightarrow c = 221 \, \frac{m}{s}$$

$$A = \pi r^2 = 3.14 \, m^2$$

$C_d = 1.42$ for $Re > 1000$

Check Re:

$$Re = \frac{\rho V 2r}{\mu} = 3.54 (10)^5$$

plug ρ, V, C_d, A into
drag equation

$\mu = 115.2$ centipoise for
CO_2 at 233 K

$\therefore C_d$ is good

$$\Rightarrow D = 603 \, N$$

III. Determination of design load to shear the pins

A. First criterion
the following inequality must be true

$$g(drag) < g(design) < g(tail)$$

$$g(drag) = \frac{D}{mg} = 4.1 \text{ g's}$$

$$g(tail) = \text{acceleration imparted by impact}$$
$$\text{of tail section} \geq 1500 \text{ g's}$$

B. Second criterion
g(drag) may be underestimated due to assumption of incompressible flow.

C. Third criterion
The shearing of the pins will send a secondary shock wave through the outer shell. This shock wave should be no greater than the primary shock wave associated with the impact of the nose.

$$\therefore g(design) \leq 400 \text{ g's}$$

Therefore,

let $g(design) = 400 \text{ g's}$

IV. Design of shear pins

$$F(design) = m \, g(design) = 110 \, kN$$

$$F(design) = Lts$$

$$S \approx 1 \, GPa$$

rewritten for square cross section

$$t = \sqrt{\frac{F(design)}{12 \, S}}$$

$$\Rightarrow t = 2.98 \, mm$$
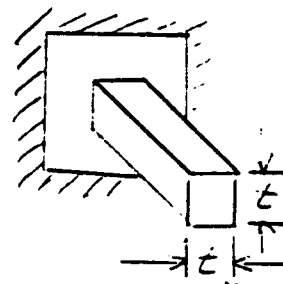
V. Determination of thickness of inner cylinder, d
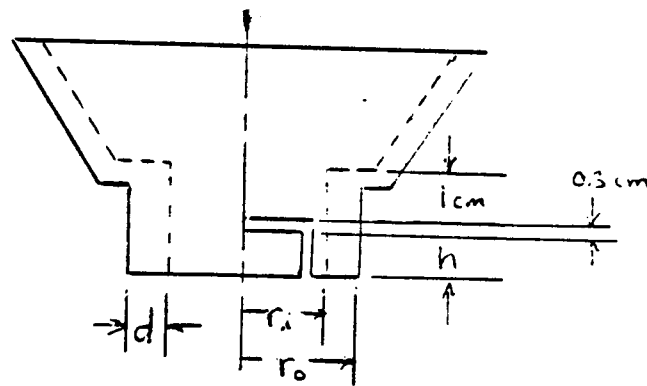
$$d = r_o - r_i$$
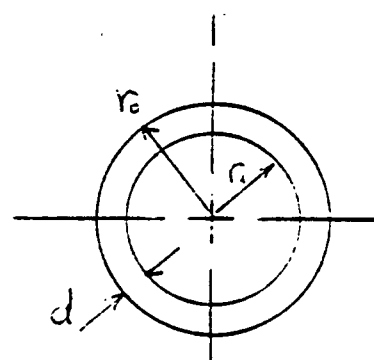
General Configuration
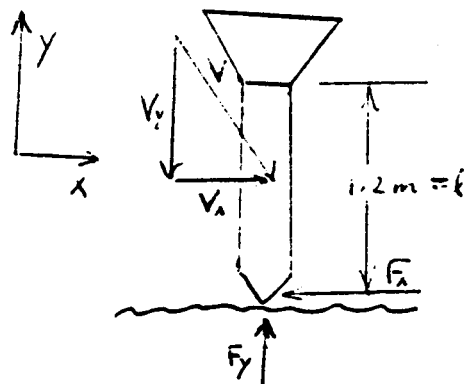
Inner shell must have thickness sufficient to resist bending due to lateral penetrator velocity at impact

Bending moment on inner shell : $M = F_x \cdot \ell$

$$V_y = 100 \ \tfrac{m}{s}$$
$$V_x = V_{wind} = 10 \ \tfrac{m}{s} \qquad \text{worst case}$$

$$F_y = ma = 58.9 \ kN$$

assume $F_x \propto F_y$ in velocity

$$\Rightarrow F_x = \frac{V_x}{V_y} F_y = 5.89 \ kN$$

F_x and F_y act at the tip of the nose cone.

Find the equivalent force - moment system acting on the inner cylinder

$$M = F_x \ell = 7070 \ N \cdot m$$
$$F_m = \frac{M}{0.0067 m} = 1.05(10)^6 \ N$$

(see diagram on following page)
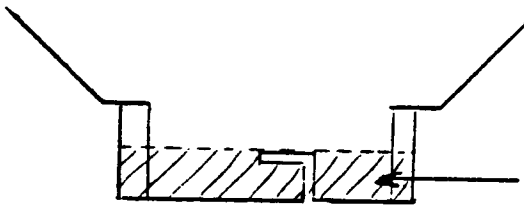
This section is weakened by the pin slots and will not be relied upon to resist bending load

$\therefore$ the equivalent force system is a combination of F_x and F_M

afterbody

1cm

F_x

+

0.5 cm

A

afterbody

F_M

A

0.333cm
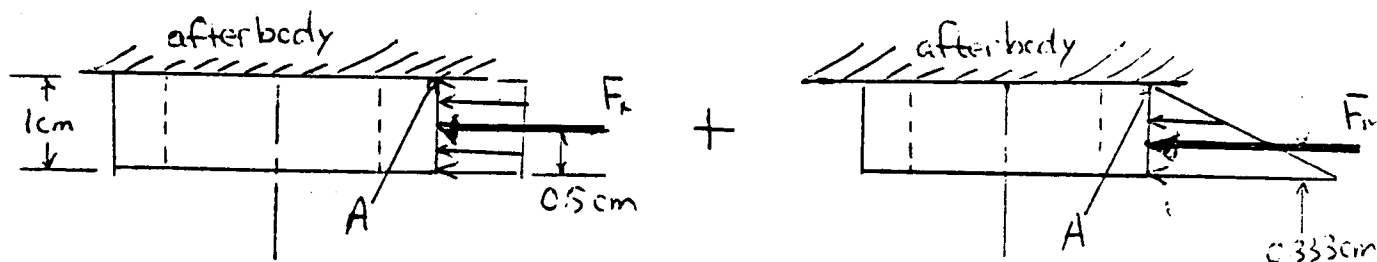
A is the point of maximum tensile stress

From elementary beam theory

$$\frac{\sigma_A}{F.S.} = \left(\frac{My}{I}\right)_{F_x} + \left(\frac{My}{I}\right)_{F_M}$$

let F.S. = 1.5

$\sigma_A = \sigma_y = 827 \text{ MPa}$

$I = \frac{\pi}{4}(r_o^4 - r_i^4)$

$y = r_o$

$\Rightarrow r_i = 4.50 \text{ cm}$

$\therefore d = 0.75 \text{ cm}$

Dimensions of lower section of inner shell

Given a thickness of 0.75 cm, find height, h, to resist shearing force, P, applied by pin.

Model

FBD
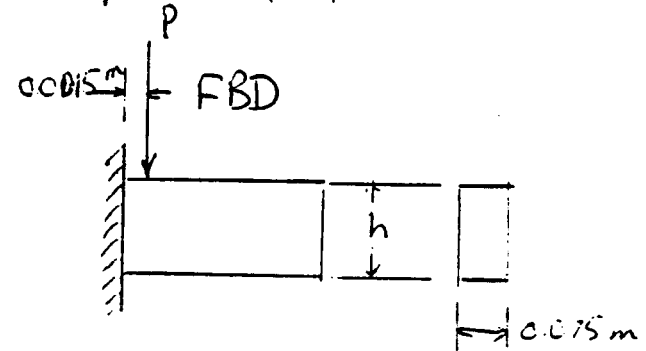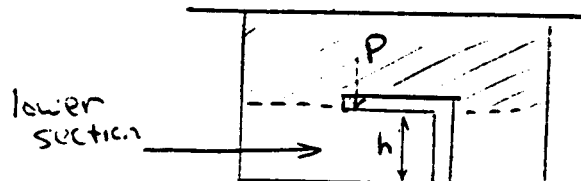
$$\sigma = \frac{F.S. \, My}{I}$$

$$\Rightarrow h = 4.89 \, mm$$

this is a minimum value

and $\tau = \frac{VQ}{It}$

$$\Rightarrow h = 0.12 \, mm$$

where: $I = \frac{1}{12}(0.75) h^3 \quad m^4$

$y = h/2 \quad m$

$M = P(0.0015) = 165 \, N \cdot m$

$P = 110 \, kN$

$F.S. = 1.5$
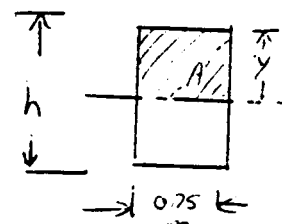
$V = P = 110 \, kN$

$\tau = \tau_y = 477 \, MPa$

$A = 0.75 \, h$

$y = \frac{h}{2}$

$I = 0.75 \, h^3$

$Q = 0.1875 \, h^2$

Therefore, height, h is determined by the size of the locking beam occupying that space.

69

II Design of locking beams

A. beam dimensions
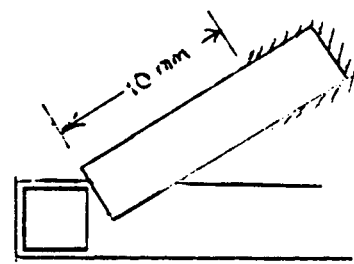
FBD
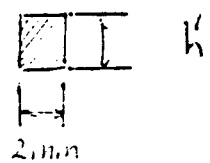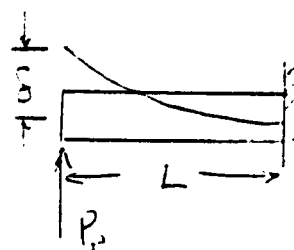
from elementary beam theory

$$P = \frac{3 \delta E I}{L^3}$$

where $c = \frac{h'}{2}$ m

$E = 107$ GPa

$I = \frac{0.002}{12} h'^3$ m⁴

$L = 0.01$ m

torque for assemby, T

$T = 3 P_p r_1$

let $T = 50$ N·m

$\Rightarrow P_p = 370$ N

$\Rightarrow h' = 1.93$ mm

B. Torque for beam failure
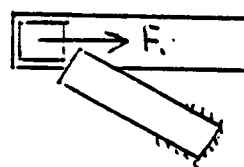
assume failure will be due to buckling
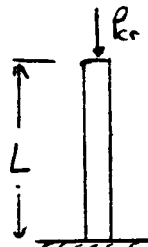
$$\sigma_{cr} = \frac{\pi^2 E}{\left(\frac{L_e}{r}\right)^2}$$

$$L_e = 2L = 0.02 \, m$$

$$r = \sqrt{\frac{I}{A}} = 5.57(10)^{-4} \, m$$

$$\Rightarrow \sigma_{cr} = 819 \, MPa$$

$$\sigma_Y = 827 \, MPa$$

$\sigma_Y \gtrsim \sigma_{cr}$ so use higher value

$$P_{cr} = \sigma_Y A = 3.27 \, kN$$

$$T_{cr} = 441 \, N \cdot m$$

NOTE:

The tolerance between the inner and outer cylinders has not been determined. Friction effects, dependent on this tolerance, have also been ignored. Friction between the cylinders will affect the torque required for assembly.   Temperature effects will be important here.

Pins have been shown planer, but must follow curvature of inner cylinder.

71

APPENDIX E.
BACKPRESSURE/ RPM TESTING RESULTS

A major problem associated with unmanned drilling is providing the correct backpressure needed to penetrate the soil. Also, since the material to be sampled cannot be chemically altered, the heat generated by drilling must be kept to a minimum. To keep the generated heat down, the drill should operate at the slowest rotational speed possible while still providing adequate cutting forces.

In order to determine the optimal combination of backpressure/rpm, a set of controlled tests were preformed. An MTS, servo-valve controlled, hydraulic testing machine was used to perform the tests. A 1000 lb load cell, operating in 10% range (100 lb max), gave an output resolution of ± 0.01 pounds. Load control was used to approximate the condition of the actual spring driven system we developed. Since the spring load will vary over the 4 cm drilling distance, test results would imply the 'average load' for the system.

A drill press was secured to the load frame of the machine. A common, variable speed drill was mounted in the frame, and aligned with the hydraulic ram. The load cell was then attached to the back of the drill, directly in line with the drill bit. The sample was then placed on the ram. This way, the load was applied by moving the sample up toward the drill bit. The load is then measured as the resultant force on the ram.

The tests included varying the rpm of the drill until a noticeable cutting rate was achieved. This rate (360 rpm) was measured by directing a strobe light on a marked portion of the bit. The load was then applied and held constant for four minutes. The load was varied from 10 to 50 pounds in 10 pound increments. For each load, the same drill bit was used to run four separate tests. Only one bit was used for each load to minimizing error due to dulling of the bit.

Our experimental data is not without error. The sharpness of the bit, degree of heat generation, and the exact hardness of the material will all effect the results. Still, we are confident in assuming that an average spring load of 30 pounds will be sufficient for soil collection.

PARABOLIC FIT TO DRILL DATA
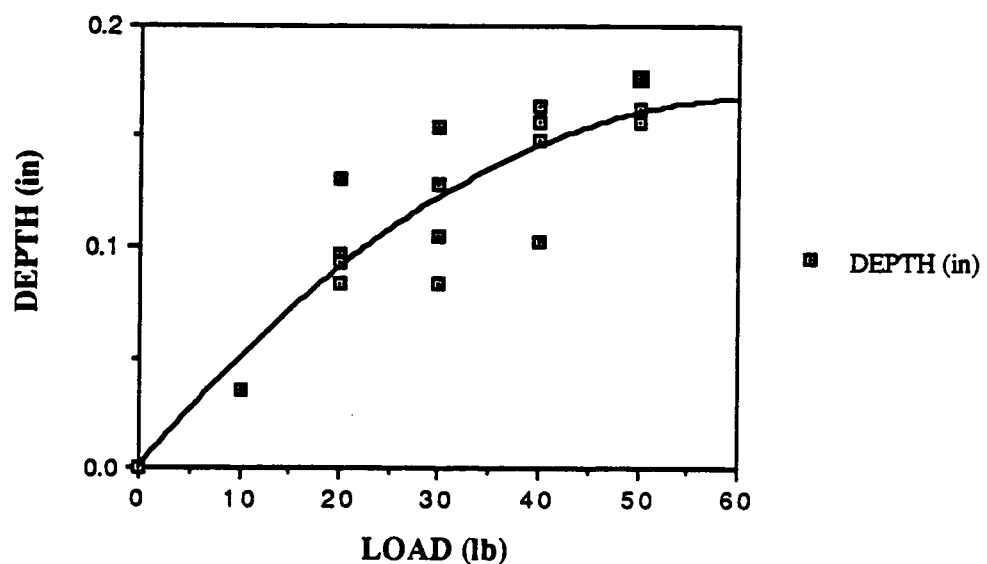
drill data

	1	2
	LOAD (lb)	DEPTH (in)
1	10	0.0348
2	20	0.131
3	20	0.084
4	20	0.097
5	20	0.093
6	30	0.154
7	30	0.128
8	30	0.105
9	30	0.083
10	40	0.148
11	40	0.157
12	40	0.163
13	40	0.102
14	50	0.156
15	50	0.176
16	50	0.162
17	0	0.00

Appendix F
Mass Allocation Chart

ITEM	MASS [gm]
Bit	
• Inner	6.4
• Outer	4.5
Driving Plate	21.0
Gear Box	110.0
Motor	300.0
PIMP	13.4
Plates	386.4
Plug	2.0
Springs (driving, plug & U-Lever)	2.0
Track	30.7
Tray and Chute	1.3
U-Lever	1.8
Total	889.5 gm

Appendix G
Heat Transfer Analysis [using FEHT by S.E. Klein, professor UW-Madison]
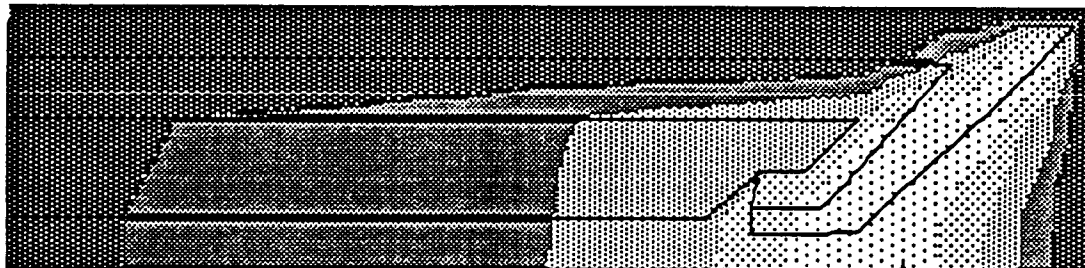
Steady-State|-40 ▆ -32 ▆ -24 ▦ -16 ▦ -8 ▦ 0 °C

TEMPERATURE CONTOURS

-40.0	-40.0	-40.0	-40.0	-40.0	-40.0	-40.0	-40	-40.0	-40.
7	-39.7	-39.6	-39.6	-39.4	-39.3	-39.2	-36.7	20.5	0 -40.
-32.7	-31.9	-30.2	-27.9	-24.5	-20.6	-17.2	-3.3	0.0	-20.4
7	-32.1	-30.9	-28.8	-25.8	-21.8	-17 -16	-1.8	0.0 -13.5	-40.0
-32.3	-31.4	-29.8	-27.1	-23.4	-17.7	-7.5 0	-4.9 15.1		-40.0
.5	-31.9	-30.6	-28.4	-25.3	-20.9	-15. -8. -2.3	-9.2	-27.6	
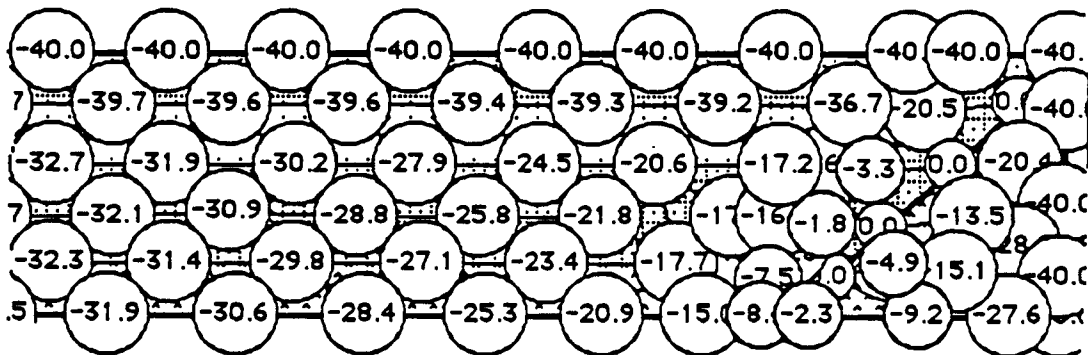
NODAL TEMPERATURES
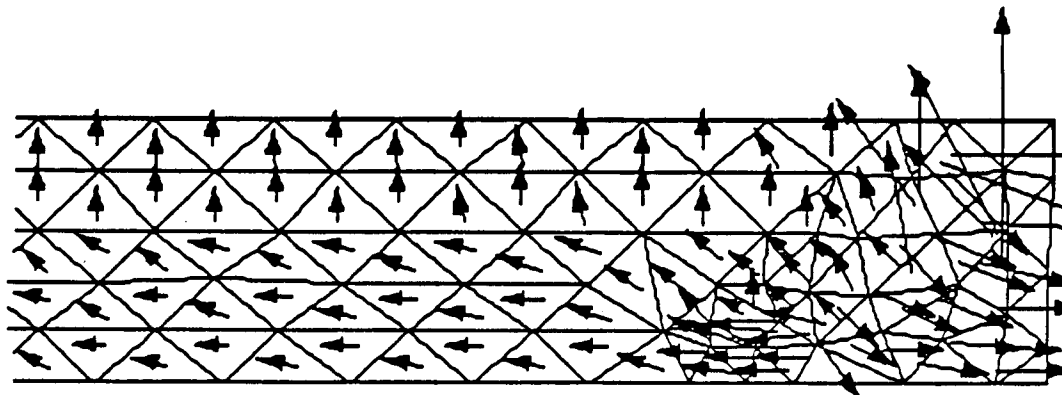
Steady-State|➤ 146.7 ─────────➤ 76386 [W/m2]

FLUX DIRECTIONS

75

APPENDIX H
BIOGRAPHIES

Mark Chun
     Project Focus : SAD Deployment
     Major : Engineering Mechanics - Aerospace
     Graduation Date : December 1988
     Post Graduation Plans : Graduate Studies in Astronomy / Physics
     Address : 1518 Jefferson Street, Madison, Wisconsin 53711

Christine Eble
     Project Focus: Sample Placement
     Major : Engineering Mechanics - Aerospace
     Graduation Date : May 1988
     Post Graduation Plans : Employment in Aerospace Industry
     Address : 201 South Mills, Apt #1, Madison WI, 53715

Thomas Kilinski
     Project Focus : Sample Gathering / Collecting
     Major : Engineering Mechanics - Composite and Experimental
     Graduation Date : May 1988
     Post Graduation Plans : Graduate Studies in Experimental Mechanics
     Address : 2501 North 28th Avenue, Wausau, Wisconsin 54401

Michael Kuehner
     Project Focus : Sample Gathering and SAD Deployment
     Major : Engineering Mechanics - Aerospace
     Graduation Date : May 1988
     Post Graduation Plans : Design and Development in Aerospace Structures
     Address : 202 South Columbus Drive, Marshfield, Wisconsin 54449

Mark Wallat
     Project Focus : SAS Suspension System
     Major : Engineering Mechanics - Aerospace
     Graduation Date : December 1988
     Post Graduation Plans : Employment in Aerospace Industry
     Address : 1017 Oakland Avenue, Madison, Wisconsin 53711

Andrew Zerfas
     Project Focus : Forebody - Afterbody Coupling
     Major : Engineering Mechanics - Aerospace
     Graduation Date : May 1988
     Post Graduation Plans : Graduate Studies in Astronautics
     Address : 906 West Sixth Street, Marshfield, Wisconsin 54449

Special Thanks to Catherine Meyer for design of the logo.

APPENDIX I
BIBLIOGRAPHY

Barns, C.E.,"Mars Penetrator Umbilical", NASA AMES.

Baumeister, Theodore and Marks, Lionel, eds. Standard Handbook for Mechanical Engineers, 7th edition McGraw Hill Book Co. NY, 1967.

Beer, Ferdinand P. and Johnston,E. Russell Jr., Mechanics of Materials, McGraw Hill, Inc.,1981.

Blanchard,M.B., and Shade, H.D., "The Effect of a Planetary Surface Penetrator on the Soil Column Surrounding the Impacting Body", NASA TM X-62428, 1975.

Brandt, John C, and McEllroy, Michael B.,eds. The Atmospheres of Venus and Mars, Gordon and Breach, Science Publishers Inc. 1968.

Carlson, Harold, Spring Designer's Handbook, Dekker Inc., New York, 1978.

Fox, Robert W., and McDonald, Allen T., Introduction to Fluid Mechanics, 3rd ed., John Wiley and Sons, 1985.

Giesecke, Fredrick E.; Mitchell, Alva; Spencer, Cecil Henry; Hill, Van Leroy and Dygdon,John Thomas,Technical Drawing, McMillian Publishing Co., Inc., 1980.

Hibbeler, R.C., Engineering Mechanics, Dynamics, McMillan Publishing Co.,1986.

Hughes Aircraft Corp., Pioneer Mars Surface Penetrator Missions, Mission Analysis and Orbiter Design.

Hunt, G.E., and Kondratyeu, K.Y., Weather and Climate on Planets, Pergammon Press, Oxford 1982.

Mash, Donald, R., Material Science and Technology for Advanced Applications.

Mckay, C.P., "Exobiology and Future Mars Missions: The Search for Mars' Earliest Biosphere", NASA Ames, 1987.

McKay, C.P., Space and Planetary Environments Criteria Guidelines for use in Space Vehicle Development, Editors Smith and West, 1982 Revision (Vol. 1).

Pao, Y.H., "Dynamical Stress Concentrations in an Elastic Plate", Journal of Applied Mechanics, **29**, 1962, p. 299+.

SAE HS J795, Design and application of Helical and Spiral Springs, SAE Information Report, Publishers' Choice Mfg. Co., Mars, 1982.

Squyres, S.W. and Ballhaus, W.F., Comet Nucleus Penetrator, Vol.1 : Investigation and Technical Plan, 1985.

Stark, L.E., "Weldability of Ti - 7Al - 2Cb - 1Tu Plate", Welding Research Supplement, Febuary 1966, pp. 70s-81s.

Swenson, B.L., McKay, C.P., and Carle, G.C., "A Preliminary Study of a Mars Penetrator System for Subsurface Exobiological Exploration", NASA Ames (IAF-87-434).

Thomson, William T., Theory of Vibration with Applications, Prentice-Hall, Inc., 1981.

Titanium Alloys Handbook

Weast, Robert C., Ed, in Chief, CRC Handbook of Chemistry and Physics, 64th ed., CRC Press Inc., 1983.

Weidner, Richard T., Physics, Allyn and Bacon Inc., 1985.